ORIGINAL ARTICLE

The machinability of titanium alloy thin-wall parts in cooling minimum quantity lubrication (CMQL) environments

Ge Wu[1] · Xuanyu Mao[1] · Wencheng Pan[2] · Guangxian Li[1,3] · Songlin Ding[1]

Abstract

The machining of thin-wall components made of titanium alloys is challenging because the poor machinability of the material leads to severe problems such as accelerated tool wear and poor surface quality, while the weak rigidity of the thin-wall structure results in unavoidable vibration and surface form errors. To address these issues, this paper investigated the mechanisms and performance of cooling minimum quantity lubrication (CMQL) in milling titanium thin-wall parts. To verify the efficiency of CMQL, different cooling/lubrication strategies, including conventional flood cooling, minimum quantity lubrication (MQL) and CMQL with different temperature levels, were investigated. The cutting force, tool wear state, chip formation, surface integrity, and surface form errors were compared and analysed in detail. The experiment results show that MQL is inadequate at higher spindle speeds due to its ineffective cooling capacity and weakened lubrication ability. In contrast, CMQL has demonstrated its feasibility and superiority in milling titanium thin-wall parts under all conditions. The outcomes indicate that a lower temperature level of CMQL is advantageous to producing better wear resistance and lower thermomechanical loads, and the CMQL (− 15 ℃) machining environment can remarkably improve the overall machining performance and control the surface form errors of the machined thin-wall parts. At the spindle speed of 3000 rpm, the surface roughness measured under CMQL (− 15 °C) condition is reduced by 16.53% and 23.46%, the deflection value is decreased by 54.74% and 36.99%, while the maximum thickness error is about 53.51% and 20.56% smaller in comparison to flood cooling and MQL machining. In addition, CMQL is an economical and sustainable cooling/lubrication strategy; the outcomes of this work can provide the industry with useful guidance for high-quality machining of thin-wall components.

Keywords MQL · CMQL · Thin-wall · Machining · Titanium · Lubrication

1 Introduction

Super alloys such as titanium-based alloys are widely used in the aerospace, biomedical and manufacturing industries owing to their superior properties such as high strength-to-weight ratio, high wear and corrosion resistance, and outstanding biocompatibility [1]. However, these alloys are also considered difficult-to-machine materials due to their low thermal conductivity, high chemical reactivity and work hardening, which consequently led to excessive cutting loads and tool wear during the machining process, as well as the poor surface quality of the machined part [2]. The machinability of titanium thin-wall components is further limited due to the weak stiffness and rigidity of the workpiece, as the machining is normally accompanied by vibration issues and surface form errors [3–5].

A large number of thin-wall machining strategies have been proposed to obtain a chatter-free process and better error control performance. The development of chatter or error prediction and compensation schemes is the major approach that is applied to overcome the challenges occurred in machining flexible thin-wall components, and great contributions to the analytical and experimental studies have been demonstrated in the literature [6–8]. To accurately describe the dynamic milling system, flexible models and

✉ Guangxian Li
  ligx0313@163.com

✉ Songlin Ding
  songlin.ding@rmit.edu.au

1 School of Engineering, RMIT University, Victoria, Australia

2 Centre for Precision Technologies, School of Computing and Engineering, University of Huddersfield, Huddersfield, UK

3 College of Mechanical Engineering, Guangxi University, Nanning, China

complex analytical solutions are normally employed, and various factors such as the tool/part deflections [9–11] and dynamic process characteristics [12–14] are considered. However, taking into account the complicatedness associated with the thin-wall milling process, the proposed analytical and numerical methods are normally time-consuming and error-prone, which restricts their application in industrial practices.

Apart from developing comprehensive analytical models, the application of metalworking fluid (MWF) is another commonly used strategy in the metal cutting process to improve the machining quality. In the machining of titanium components, a large amount of cutting heat is produced and cumulated in the cutting area due to high cutting loads, low thermal conductivity of the base material and increased adhesion wear caused by the enhanced chemical reactivity of titanium toward the tool material at elevated cutting temperatures [15]. Therefore, the use of MWF is highly desired to minimise these issues. The conventional flood cooling method is the most general way of using MWF in manufacturing operations. However, cutting fluid ejected in the flood cooling process may fail to penetrate the cutting zones due to excessive cutting loads in high-speed machining of titanium alloys [16]. Meanwhile, the machining cost, environmental and health hazards associated with the usage of typical MWF have also resulted in growing concerns [17]. To achieve a cleaner production process, several green manufacturing technologies, such as minimum quantity lubrication (MQL), cryogenic/cooling minimum quantity lubrication (CMQL) and nanofluid minimum quantity lubrication (NMQL), have been developed to effectively enhance the machining performance and minimise hazards.

As an environment-friendly process, MQL involves the atomisation and ejection of a very small amount of MWF. While the consumption of MWF in MQL is about ten-thousandth of the amount applied in the flood cooling machining [18], the overall machining quality can be improved to a certain extent. Various experimental studies on MQL machining are reported in the literature, and the majority of these studies are focused on the optimisation of MQL parameters as well as the types of coolant. For instance, Liao et al. [19] investigated the feasibility of MQL in high-speed milling of NAK80 hardened steel with different oil viscosities, cutting speeds and feed rates. The results show that MQL improved tool life and surface quality under all cutting conditions when compared to dry and flood cooling experiments. Li and Chou [20] analysed the influence of different MQL parameters in near micro machining of SKD 61 steels and found that the effect of air flow rate on tool life was more significant by increasing the penetration ability of the oil drops. Later, Fratila and Caizar [21] optimised the cutting and MQL parameters in face milling by using the Taguchi optimisation methodology.

Although the effectiveness of MQL has been demonstrated in plenty of studies, some researchers also found that the machinability of MQL is limited in high-speed machining of difficult-to-machine materials due to the insufficient cooling capacity of the airflow, which may result in relatively larger cutting forces, excessive cutting temperature and failure of lubrication function. For instance, Yuan et al. [22] pointed out that conventional MQL has a slight influence on the reduction of cutting force and flank wear in milling of Ti-6Al-4 V, and a worse surface finish was obtained compared with cooling MQL machining. Work conducted by Leppert [23] also showed that the application of MQL did not have a considerable influence on the resultant force in turning of C45 steel due to weakened lubrication and cooling functions.

As an improvement of traditional MQL machining, CMQL is enhanced by introducing a compressed sub-zero airflow [24, 25] or other cryogenic mediums (e.g. nitrogen [26], liquid nitrogen (LN$_2$) [27–29], supercritical CO$_2$ (scCO$_2$) [30, 31]) together with the MQL mist flow. This hybrid method which combines the advantages of MQL and cryogenic machining can eliminate the limitations of MQL by significantly increasing the heat transfer efficiency at the cutting area. It has been reported that CMQL helps to promote the machining quality and productivity when compared to other cooling/lubrication strategies. In the work of Sun et al. [32], cooled compressed air was delivered to the tool rake and flank faces in turning of Ti-6Al-4 V. The effect of the cryogenic compressed air leads to decreased cutting temperature and thereby a reduction of built-up edge (BUE) as well as tool wear. Zhang et al. [33] evaluated the cutting performance of CMQL in enhancing the machinability of Inconel 718. They have shown that the application of CMQL can significantly improve the tool wear state, and cleaner manufacturing of Inconel 718 can be obtained. Furthermore, the effect of the sub-zero air (− 10 °C) was examined in the milling of Ti-6Al-4 V [34]. It was demonstrated that the introduction of cold air could efficiently solve the thermal issue that occurred in high-speed machining of titanium alloy by increasing the surface heat transfer coefficient and reducing the cutting loads. More recently, Bagherzadeh et al. [35] investigated CMQL machining by spraying liquid nitrogen and carbon dioxide in slot milling of Ti-6Al-4 V. The effectiveness of this hybrid cooling technique has been demonstrated in terms of tool life, cutting force/temperature and surface quality. And it was proved that this hybrid method is more effective at higher cutting speed.

However, despite the considerable research regarding the optimisation of thin-wall machining and the performance of MQL/CMQL technologies, there are only a few investigations on the cooling/lubrication strategies in thin-wall milling, and there is still a knowledge gap in identifying the effects and effectiveness of MQL/CMQL in the titanium

thin-wall milling process. This paper is dedicated to improving the machinability of titanium thin-wall components and investigating the performance of MQL/CMQL in machining titanium thin-wall components by analysing the experimental results obtained under different machining conditions. The cutting force signal, tool wear state, surface integrity, and surface form errors are considered as the machinability indicators. The mechanisms and the specific role of CMQL in thin-wall machining are comprehensively discussed and compared with other cooling/lubrication strategies. The results prove that CMQL machining can significantly improve the efficiency and quality while reducing the surface form errors in titanium thin-wall machining. The outcomes of this work can provide the industry with useful guidance for high-quality thin-wall machining, and the implementation of this sustainable machining strategy can promote a more comprehensive application of titanium thin-wall components in industries.

2 Experimental procedures

The thin-wall milling experiments were conducted on a Haas 3-axis vertical machining centre equipped with a multi-nozzle flood coolant system. In flood cooling machining, high-volume MWF is delivered to the cutting zone to flush out chips and maximise the machining efficiency. The workpiece was clamped on a Kistler 9119AA2 multi-component dynamometer, and this dynamometer was mounted on the machine worktable. During the cutting process, the milling force components were measured by this piezoelectric dynamometer with a sampling rate of 50 kHz. The recorded signals were amplified and transferred through the data acquisition unit (Kistler LabAmp Type 5165A) and eventually visualised by the Kistler DynoWare software. To avoid any deviation and ensure the accuracy of the milling process, the straightness of the fixed thin-wall part was checked along the feed direction before the machining. The real-time deflection values of the machined thin walls were measured by three non-contact displacement sensors (Lion precision ECL 130) that were mounted along the feed direction with an equal interval of L/2 ($L1 = 0$, $L2 = 1/2\ L$ and $L3 = L$, L is the length of the thin wall). The acquired data was then analysed by the LabVIEW software. The experimental setup is shown in Fig. 1.

In this study, the titanium alloy Ti-6Al-4 V was used as the workpiece material. The physical properties and chemical compositions of Ti-6Al-4 V are listed in Tables 1 and 2 respectively.

The blocks of raw Ti-6Al-4 V were pre-machined to desired thin-walled parts with overall dimensions of 80 mm (L) × 30 mm (W) × 36 mm (H); the height and initial thickness of the thin walls are 26 mm and 3 mm, respectively. Four-flute solid tungsten carbide end mills (Guhring no.
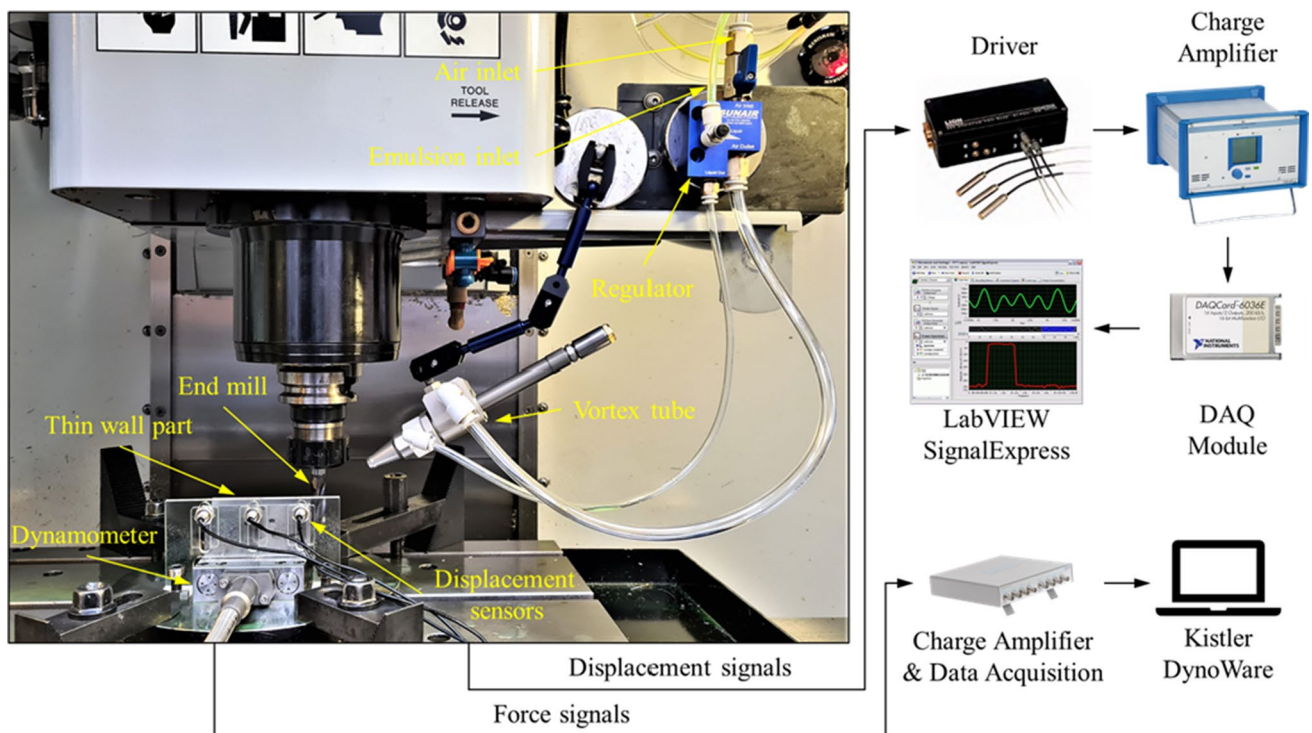

Fig. 1 Experimental set-up

**Table 1** Physical properties of Ti-6Al-4 V [36]

Yield stress (MPa)	Tensile strength (MPa)	Hardness (HV_{20})	Poisson's ratio	Thermal conductivity at 20 °C (W/mK)	Modulus of elasticity (GPa)	Density (g/m³)
745	832	600	0.34	6.60	113	4.50

Table 2 Chemical compositions of Ti-6Al-4 V [37]

Al (%)	V (%)	C (%)	Fe (%)	O (%)	N (%)	H (%)
5.50~6.75	3.50~4.50	0.10	0.30	0.20	0.05	0.013

Table 3 Milling parameters

Feed per tooth f_z (mm/z)	Spindle speed n (rpm)	Cutting velocity V_c (m/min)	Axial depth of cutting a_p (mm)	Radial depth of cutting a_e (mm)	Machining environments
0.06	1500–3000–4500	56.55–113.10–169.65	25	0.50	Flood, MQL, CMQL

Fig. 2 Schematic of the MQL/CMQL system
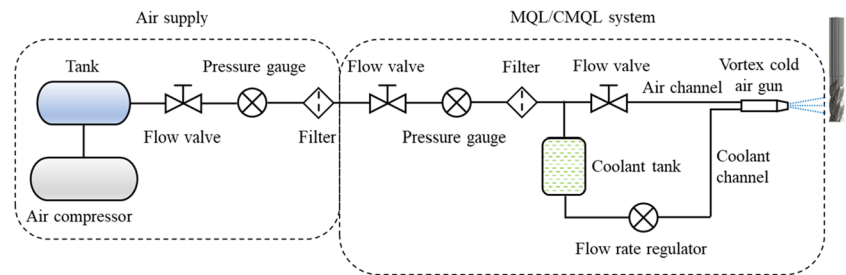
3562 and Standard DIN 6527 L) with a diameter of 12 mm, a helix angle of 30°, and a cut length of 26 mm were used for the peripheral milling experiments. To minimise the influence of tool wear on overall machining performance, a new end mill was used for each cutting trial. Moreover, the tool overhang from the tool holder to the tool tip was checked and fixed to reduce the influence of tool vibration and runout.

The cutting parameters of the peripheral down milling process are selected based on our previous work [38] and listed in Table 3. In this study, different machining environments including flood cooling, MQL and CMQL with different temperature levels were applied and investigated as the variables. Spindle speed also is a variable as it could influence the penetration condition of different cooling/lubrication strategies and affect the machining performance.

In flood cooling machining, the conventional emulsion coolant and flexible coolant hose were used for the supplying of low-pressure MWF flow during the machining. While in MQL and CMQL machining, a dual-channel system (Fig. 2) was used to produce a room-temperature mixture flow in MQL and a sub-zero mixture flow in CMQL. In this system, the airflow is compressed and filtered before entering the main pipeline. Then, a smaller fraction of the compressed air is transferred to the coolant tank to drive the emulsion

coolant, and a continuous coolant flow is delivered to the cutting area in the form of an atomized spray through the nozzle. If the CMQL machining is applied, a large volume of compressed air will be transported to the vortex cold air gun through another channel. The cold air gun will be activated and produce a refrigerated airflow with a temperature range from 0 to − 15 °C by adjusting the input airflow rate and pressure. The sub-zero airflow and the coolant flow from separate channels are then mixed within the mixing chamber of the cold air gun. As the flow rate and pressure of the compressed airflow are much higher than the coolant flow, the emulsion coolant is atomized and broken into a large number of micro droplets and then ejected to the cutting area to perform the cooling and lubrication functions. Both the cold air gun and the adjustment module can be mounted on the specialized fixture or the machine enclosure by the magnetic base. And the position and angle of the nozzles can be flexibly adjusted to ensure the mixture flow can be accurately ejected to the cutting area. In this study, the temperature values of the mixture flow were measured by a wired digital thermometer, which is suitable for air or liquid measurement within an ambient temperature range of − 30 to + 50 °C. Before each experiment, the temperature of the mixture flow was measured by the type K temperature probe,

Table 4 MQL and CMQL parameters

Nozzle distance (mm)	Nozzle angle (°)	Pressure (MPa)	Flow temperature (°C)
20	45	6.90	20, − 5, − 10, − 15

and the temperature was controlled by carefully turning the adjustment knob at the end of the vortex tube until a stable mixture flow with desired temperature value was obtained. The MQL/CMQL parameters used in this study are listed in Table 4.

After each cutting trial, the used end mill and generated chips were collected and cleaned ultrasonically in ethanol for further observation. The worn tools were observed and characterised by the Leica EZ4 HD stereo microscope and FEI Quanta 200 scanning electron microscope (SEM). As the surface integrity was considered an evaluation factor, the machined thin walls were wire-cut off from the base material and then observed by using SEM to examine micro defects. The Alicona optical 3D measurement device was used to analyse the surface profile and burr formation. In addition, the surface roughness was measured using a TIME3221 Surface Roughness Tester. The assessment length is 12.5 mm, and the sampling length is 205 mm in each measurement. To ensure accuracy, the measurement was repeated five times for each sampling area, and the averaged measurement was used for further analysis.

3 Results and discussion

3.1 Evaluation of cutting force signals

The normal force component F_y perpendicular to the feed direction has more significant impacts on the part deflection and vibration. Therefore, the acquired normal cutting force signals are analysed in both the time and frequency domains to investigate the performance of different cooling/lubrication strategies.

Figure 3 displays the average values of peak cutting force components that were measured under different machining environments. To avoid the influence of the instantaneous engagement and transient vibration that occurred at the cut-in stage, only the signals measured within the stable stage were considered.

According to Fig. 3, it can be seen that the largest cutting force occurred in flood cooling machining, and the cutting forces gradually decline with a reduction of the CMQL temperature; the MQL can be regarded as CMQL but at room temperature. The decreasing force signals indicate that promoted cooling and lubrication effects were obtained when the refrigerated mixture flow was introduced into the cutting
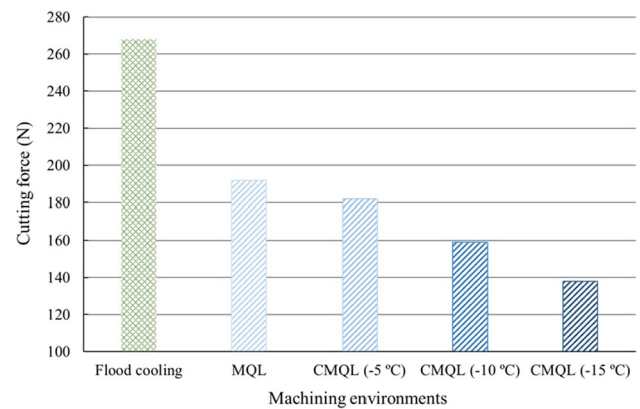

Fig. 3 Cutting forces under different machining environments ($f_z =$ 0.06 mm, $Vc = 113.10$ m/min, $a_e = 0.50$ mm, $a_p = 25$ mm)

area. And this improvement can be attributed to the efficient atomization and enhanced penetration ability of the micro droplets (with smaller diameters and higher velocities) because of the larger flow rate and pressure in CMQL [39], weakened material adhesion at lower cutting temperatures [40] and better tribological characteristics (i.e. adsorption and load-bearing capacities) due to increased viscosity of the MWF [34]. The noticeable higher cutting force measured in flood cooling was attributed to the inadequate penetration ability of MWF that was ejected with a smaller coolant pressure, and the MWF failed to reach the interfaces especially the tool-chip interface due to the intensive contact and shear stress [41, 42]. While in MQL, the droplets with high velocity can be effectively adsorbed on the interfaces and form a boundary lubricating film, and then rapidly spread to the difficult-to-reach areas due to the difference in local pressure and temperature. This effect was further enhanced in CMQL due to more significant velocity and temperature differences, and a maximum reduction of 48.59% was recorded with CMQL (− 15 °C) when compared to the flood cooling condition.

To evaluate the influence of spindle speed on the efficiency of different machining strategies, the average peak amplitude of the normal force component F_y measured within the stable cutting stage was calculated (as shown in Fig. 4) as the reference. Figure 4 reveals the reduction in cutting forces with the increase in spindle speeds in all cases. The rising material removal rate (MRR) and thereby the significantly increased heat generation and the enhanced thermal softening effect of the subsurface material are the primary reason leading to such variations [43].

Compared with flood cooling, better performance of MQL can be noted before the spindle speed is raised to 4500 rpm. However, at the highest spindle speed, the cutting force measured in MQL is slightly higher than in flood cooling machining. As mentioned in Sect. 2, the spindle speed
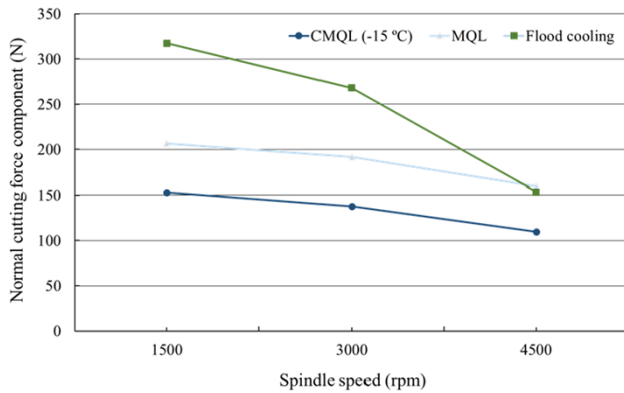
Fig. 4 Cutting forces under different cutting conditions ($f_z = 0.06$ mm, $a_e = 0.50$ mm, $a_p = 25$ mm)

Fig. 5 Frequency spectrums of cutting force signals under different machining environments ($f_z = 0.06$ mm, $Vc = 113.10$ m/min, $a_e = 0.50$ mm, $a_p = 25$ mm)

was selected as one of the variables because the high-speed rotating tool might block the MWF from reaching the cutting area and adversely influence the subsequent cooling/lubrication effects [44]. In MQL, the mist flow with a relatively lower flow rate and pressure cannot penetrate into the cutting area efficiently, and the adsorbed droplets with insufficient heat dissipation would evaporate or burn rapidly at elevated cutting temperatures. Therefore, both the cooling and lubrication functions of MQL become inadequate under high cutting speed conditions. While in flood cooling, the ejection of a large amount of MWF compensates for the diminished penetration capacity and favours continuous heat dissipation.

In contrast, the CMQL (− 15 ℃) condition demonstrated a consistent ability to reduce the cutting force regardless of spindle speed. The average cutting force is 28.47% and 31.19% lower than in flood cooling and MQL machining even at the highest spindle speed. In CMQL machining, the refrigerated and compressed mixture flow with a much larger flow rate and pressure owns a prominent heat dissipation capability due to the combined effect of reinforced convection, boiling and evaporation, which facilitate efficient heat dissipation and prevent the adhesiveness of the workpiece material. The jet impingement also contributes to breaking the vapour film that may form over the high-temperature interfaces and hinder the subsequent heat transfer process [45]. Besides, the droplets with a better penetration ability can form a more stable lubrication film after attaching over the interfaces owing to the enhanced properties of MWF at lower temperatures, which avoids direct contact between the contact interfaces and, in turn, reduces the frictional force components. Therefore, CMQL (− 15 ℃) is the most reliable strategy for reducing the cutting force especially in high-speed machining.

Prediction or detection of chatter vibration is critical in machining thin-wall components because unexpected chatter occurs frequently, and it can result in accelerated tool wear and poor surface finish. This problem becomes more
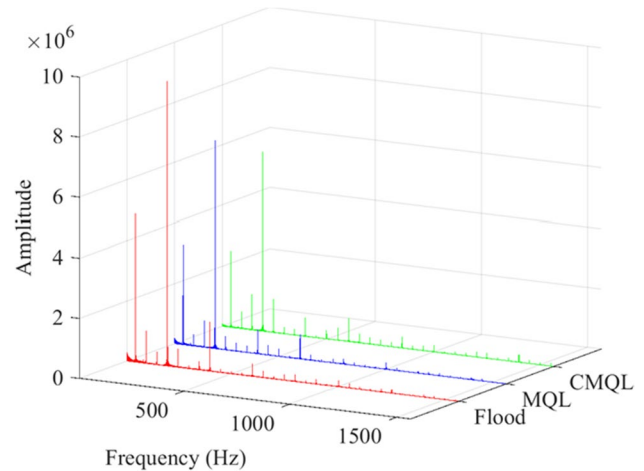
serious in machining turbine blades because the tool has to move along the specially designed tool path [46, 47]. In order to detect the occurrence of chatter, the dynamic cutting force signals in the time domain were further transferred into the frequency domain by the fast Fourier transform (FFT) method. The frequency components and spectrum characteristics are displayed and compared in Fig. 5.

From Fig. 5, it can be observed that the dominant frequency components are consistent with the spindle frequency (SF) and tooth passing frequency (TPF), as well as their subsequent harmonics. In this case, the SF is 50 Hz and the TPF is therefore 200 Hz. Meanwhile, no apparent oscillation frequency components corresponding to chatter vibration are found in the spectrum. Therefore, it can be determined that no chatter occurred, and the tool-workpiece system was stable under each machining environment. Except for the dominant frequency components, noise frequency peaks are found around the 1st SF and TPF, and these peaks are more distinct in the flood cooling condition. These peaks might be caused by the radial tool run-out and varying chip loads due to the part deflection. Figure 5 also shows a remarkable reduction in the intensity of dominant frequency peaks and noise frequency peaks from flood cooling to CMQL (− 15 ℃) condition, which means reduced cutting loads and less shear energy when removing the workpiece material in CMQL (− 15 ℃). Therefore, the milling process under CMQL (− 15 ℃) condition is more stable, which can be further verified by the corresponding time domain force signals that exhibit fewer oscillations. Reduced force and thermal variations are considered the main reason for a stable cutting process under CMQL condition.

3.2 Comparison of tool wear mechanisms

Tool wear states and mechanisms are closely associated with the efficiency of different cooling/lubrication strategies. Figures 6 and 7 display the images of the tool wear morphology on the rake and flank surfaces under various machining environments.

In general, adhesive wear on the tool rake surface and abrasive wear on the tool flank surface are identified as the dominant types of wear in all machining environments.
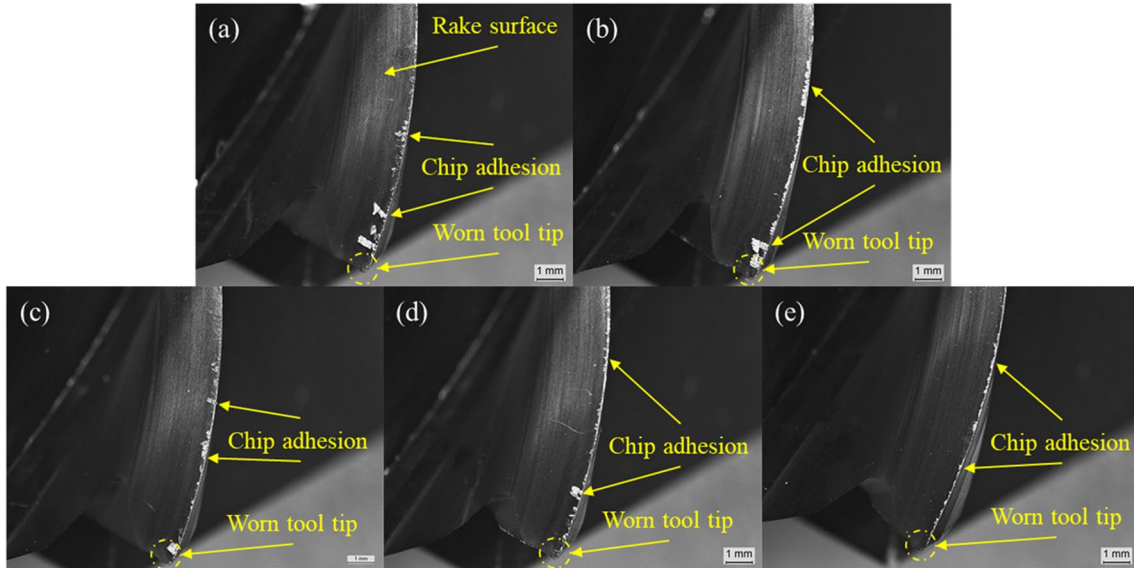

Fig. 6 Comparison of tool rake wear states under **a** flood cooling, **b** MQL, **c** CMQL (− 5 ℃), **d** CMQL (− 10 ℃), **e** CMQL (− 15 ℃) (f_z = 0.06 mm, Vc = 113.10 m/min, a_e = 0.50 mm, a_p = 25 mm)
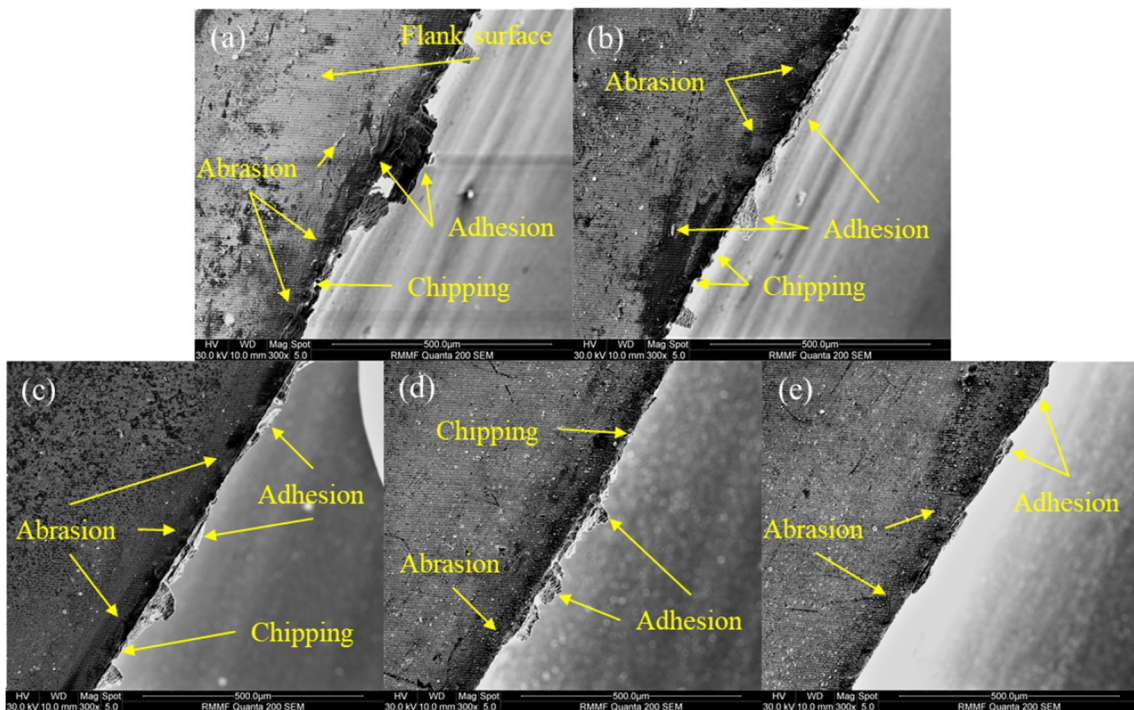
Fig. 7 Comparison of tool flank wear states under **a** flood cooling, **b** MQL, **c** CMQL (− 5 ℃), **d** CMQL (− 10 ℃), **e** CMQL (− 15 ℃) (f_z = 0.06 mm, Vc = 113.10 m/min, a_e = 0.50 mm, a_p = 25 mm)

Adhesive wear has been proved to be temperature dependent, and the strong adhesion of Ti-6Al-4 V to the carbide substrate of the cutting tool has been verified in the literature [48, 49]. Therefore, chips generated were prone to adhere to the cutting edge and machined surface because of the excessive stress and temperature in the cutting area, as well as the increasing chemical affinity of the workpiece material. From Fig. 6 a to e, the gradually reduced tendency of adhesion along the cutting edge proves that the lower temperature mixture flow can considerably enhance the cooling effect and reduce the plasticity as well as the chemical reactivity of the workpiece material owing to the enlarged temperature difference and increased heat-flux density. In addition, irregular chipping or peeling of the cutting edges was observed in the flank wear zone where part of the surface tool material had vanished. The occurrence of this abrasive wear is considered the result of thermal shock, peeling off of the welded workpiece material under excessive stress gradients and weakened strength of the cutting edge [50, 51]. From Fig. 7, it can also be found that the tool degradation certainly relates to the applied CMQL temperature level. From MQL to CMQL ($-$ 15 ℃), the tendency of adhesive wear and diffusion of the carbide end mill decreases significantly

as the refrigerated mixture flow can absorb more cutting heat through the rapid boiling heat transfer and vaporization process. Meanwhile, due to the higher flow rate and pressure in CMQL, the droplets with smaller sizes and higher velocities facilitate an effective penetration of MWF, while the superior and continuous cooling effect further strengthens the tool material and load-carrying capacity of the formed lubrication film. Therefore, smoother cutting edges with enhanced wear resistance and a noticeable reduction in abrasive wear can be noted.

The rake wear states observed under different cutting conditions are presented in Fig. 8. With the V_c of 56.55 m/min, flood cooling shows more obvious adhesion of workpiece material on the tool rake surface as compared to other machining environments. Then, the elevated spindle speed has aggravated the adhesive wear more seriously, and the formation of BUEs that adhered to the tool and resulted in a blunter cutting edge was observed at the V_c of 113.10 m/min. Hence, it is evident that the cutting temperature and heat generation increased significantly at higher spindle speeds owing to the reduced interaction period, impediment of the vapour film, diminished effectiveness of MWF and a more serious rubbing effect along the contact interfaces.
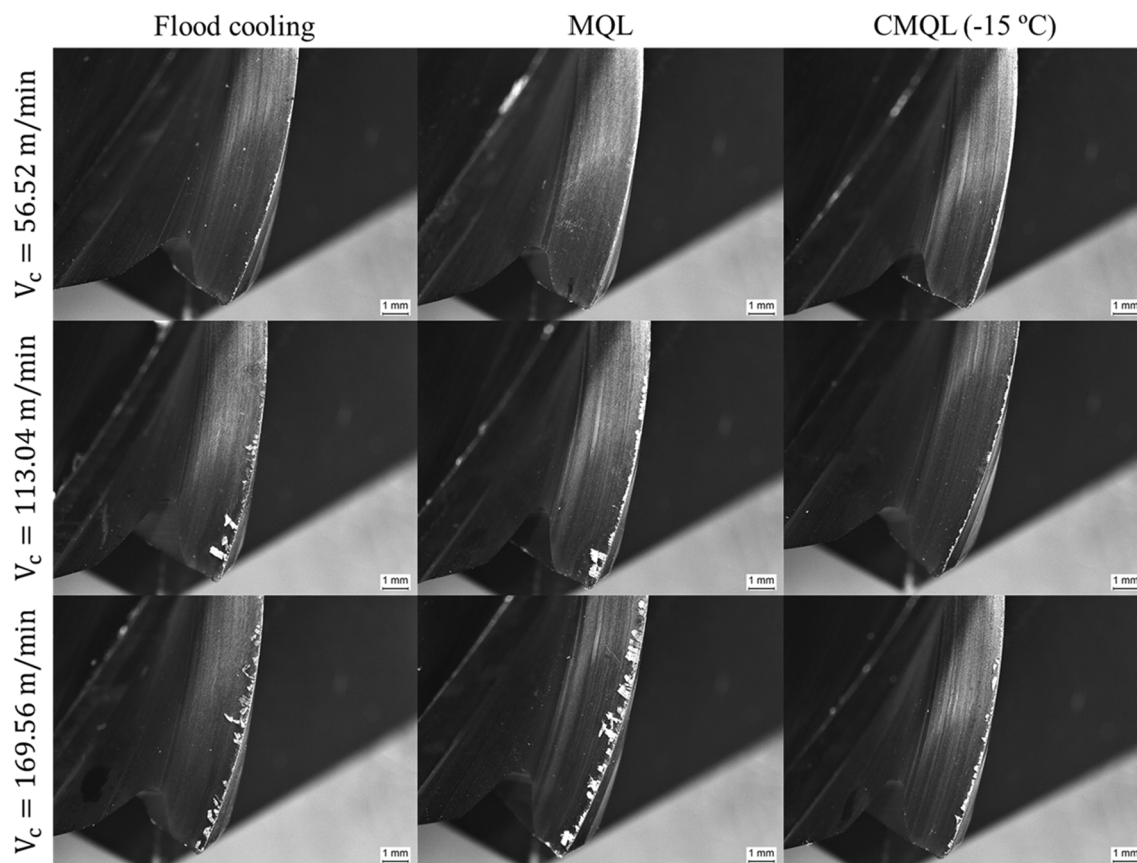

Fig. 8 Comparison of tool rake wear state under different spindle speeds (f_z = 0.06 mm, a_e = 0.50 mm, a_p = 25 mm)

Under the MQL condition with the V_c of 169.65 m/min, the optical image shows that a large amount of chips is adhered to the tool rake surface, and the wear state is worse than that in flood cooling condition, which proves the absence of cooling function of MQL at higher spindle speeds due to the poor cooling capability of air and rapid evaporation of the micro droplets. The adherent and accumulated debris will further change the tool geometry, deteriorate the contact condition, increase the thermal load and lead to an accelerated wear state and degraded surface quality in the subsequent cutting operations [52, 53]. While in flood cooling machining, less adhesion was observed under higher V_c conditions due to adequate cooling and lubrication effect provided by the bulk flow of MWF. CMQL exhibited a notable reduction of adhesiveness of the freshly machined surface and chips even at elevated V_c when compared to other machining environments, which provides strong evidence of the consistent effectiveness of the refrigerated compressed mixture flow in maintaining its cooling and lubrication performance.

The morphologies of the tool flank wear in relation to the highest V_c are also presented in the SEM images (Fig. 9). The enlarged SEM images depict that there are clearly visible adherent chips on the tool rake surface and irregular peeling or chipping on the tool flank surface in all cases. Moreover, the dark area along the cutting edge indicates the high cutting temperature and surface burning even under CMQL (− 15 ℃) condition. But it can be seen that the introduction of the micro droplets in conjunction with the refrigerated compressed flow has significantly minimized the adhesion and the maximum flank wear length in comparison to others, which supports the use of CMQL (− 15 ℃) at higher V_c range. Overall, the cooling and lubrication functions of MQL are greatly weakened at higher spindle speeds, and the worst wear condition is observed. While a substantial reduction in adhesive and abrasive wear is observed in CMQL (− 15 ℃) regardless of the spindle speed, thereby the improvement of tool life is remarkably promoted, and the total machining cost can be reduced.

3.3 Comparison of surface integrity

3.3.1 Burr formation

Burr formation in the metal cutting process is due to the combined effects of cutting actions (ploughing and extrusion), heat accumulation, plastic deformation as well as elastic recovery of the workpiece material. The existence of burrs will adversely influence the surface quality and assembly accuracy, but it cannot be completely avoided in the machining of Ti alloys because of the high thermal effect and ductility of the material.

In this study, the burrs formed along the side edge of the machined thin-wall part were observed and measured using the SEM and the Alicona optical 3D measurement device. The geometry and characteristics (burr height (b_h) and burr width (b_w)) of the burrs are presented in Figs. 10 and 11, respectively. The performance of each machining condition is analysed based on the average burr height and burr width measured from ten sampling locations along the side edge.

Due to the insufficient tool-workpiece engagement caused by the instant deformation of the thin-wall part, the cutting edge did not completely remove the chip flow generated during the cut-in stage, and as the down-milling strategy was adopted, a small portion of the workpiece material was squeezed and rubbed by the cutting edge and eventually turned into entrance burr (Fig. 10). The formation of non-uniform entrance burr was observed in all cutting trials.

The characteristics (average burr height and width) of burrs under different machining environments are given in Fig. 12. As demonstrated, at the Vc of 113.10 m/min, the largest average burr size values are measured in flood cooling machining while the smallest burr formation is found in CMQL (− 15 °C), and a reduction of the average burr size was noted when the CMQL temperature decreased. The variation of burr size could be attributed to the plastic deformation that is highly dependent on the changing thermomechanical properties (i.e., ductility, brittleness, and yield strength) of the workpiece material at different cutting temperatures [54]. With a decreasing CMQL temperature, the reduced cutting temperature would lead to a reduction of ductility and plasticity as well as an increment of the yield strength and brittleness, thereby inducing stiffer burrs with smaller burr sizes. While in flood cooling, the generated chips are bent more easily and undergo greater plastic deformation due to the higher cutting temperature. Therefore, CMQL (− 15 °C) is preferred over other machining environments when considering the control of the size and intensity of burrs.

In addition, the characteristics of burrs formed under different spindle speeds are measured and compared. From Fig. 13, it can be observed that the overall trend is that the entrance burr tends to strengthen on the side edge when the spindle speed increases from 1500 to 4500 rpm. Despite the reduction in cutting forces with increasing spindle speed, the cutting heat increased considerably due to larger MRRs and has a more significant effect on burr formation. The rising cutting temperature and associated plastic deformation capacity of the workpiece material are the major factors that influence the burr size.

Among all machining conditions, burr formation is more intensive in flood cooling and MQL machining. It can be noted that flood cooling has shown results comparable to MQL at lower spindle speed, while the thermal effect of different cooling strategies on burr size is
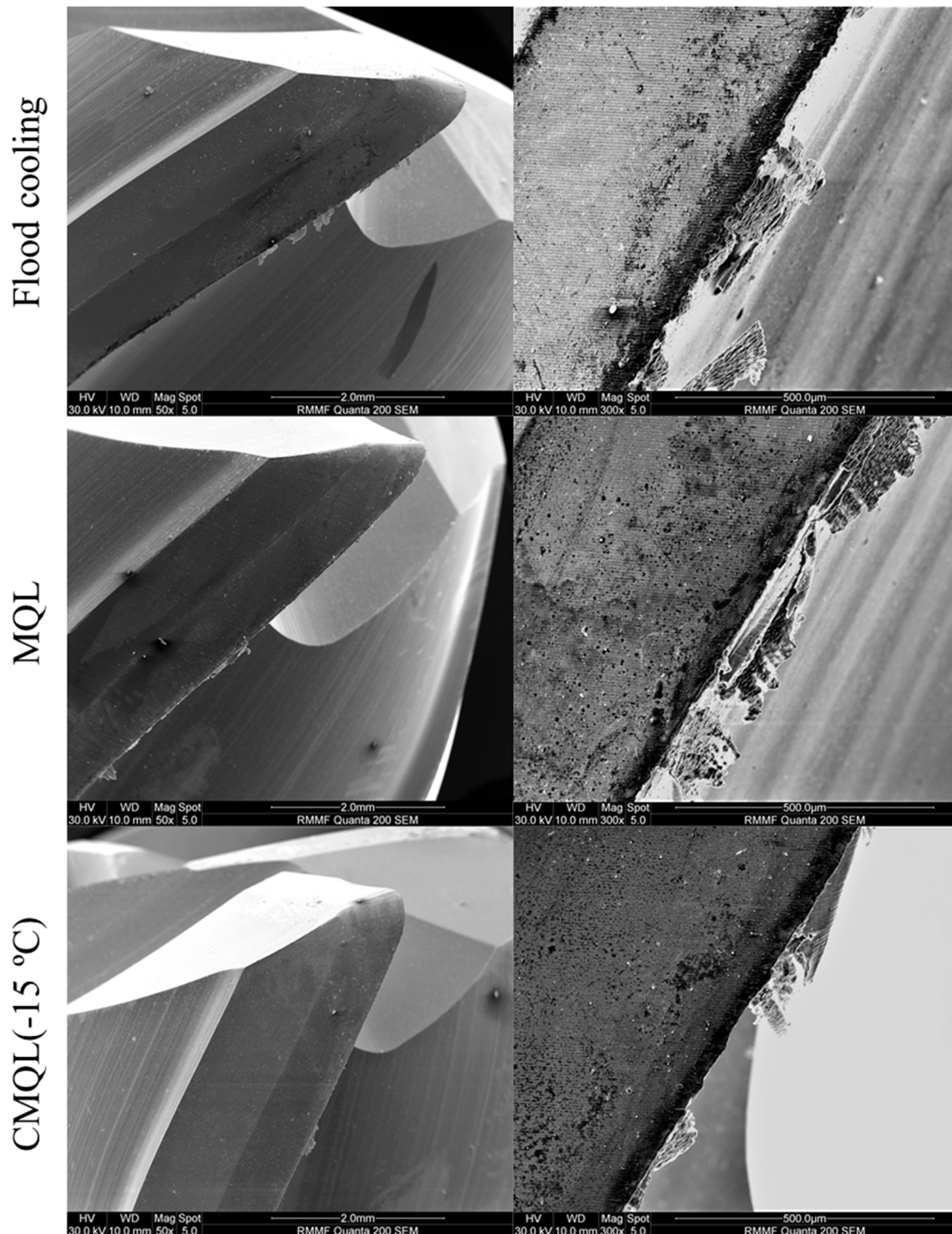
Fig. 9 SEM images of the flank wear ($f_z = 0.06$ mm, $Vc = 169.65$ m/min, $a_e = 0.50$ mm, $a_p = 25$ mm)

more obvious when milling with higher spindle speeds. Burrs were found more intensely in MQL machining at the spindle speed of 4500 rpm, and under this cutting condition, wider and flatter burrs with pit marks were found (as shown in Fig. 14). This is because of the greatly weakened

cooling and lubrication capacities of MQL at higher spindle speed due to insufficient penetration time, a smaller number of penetrated droplets and damaged lubrication film under high cutting loads, which resulted in elevated
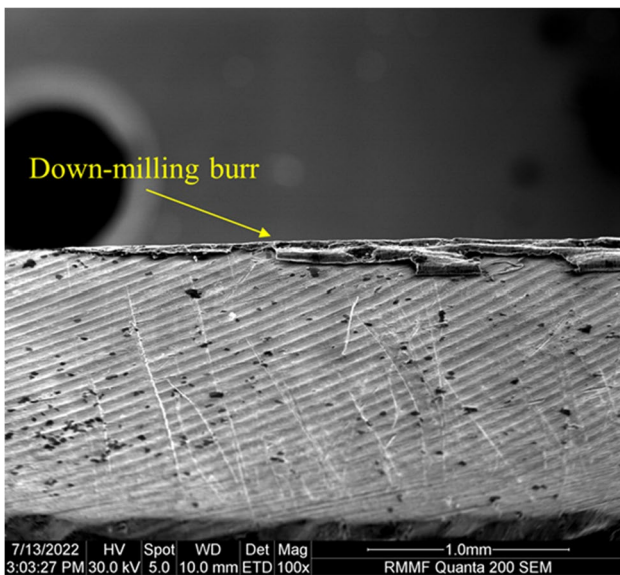
Fig. 10 SEM image of burr formation (MQL, $f_z = 0.06$ mm, $Vc = 113.10$ m/min, $a_e = 0.50$ mm, $a_p = 25$ mm)

cutting temperature in the deformation zones and growing plastic flow property of the workpiece material.

Generally, burr formation is less intensive in CMQL (− 15 °C) as compared to others, irrespective of spindle speeds. Burrs formed in CMQL (− 15 °C) were tiny and sparse, and the burr size did not change much with

increasing spindle speed under this machining environment. Under the cutting condition of CMQL (− 15 °C) combined with the spindle speed of 4500 rpm, the average burr width was reduced by 48.05% and 49.46% in comparison to the flood cooling and MQL machining, respectively. The efficiency of CMQL (− 15 °C) in reducing the formation of burrs also proves that CMQL (− 15 °C) has obvious advantages in reducing the cutting temperature due to its enhanced cooling ability and stable lubrication performance.

3.3.2 Surface roughness and defects

Surface roughness largely affects the mechanical properties of the machined part, such as fatigue strength, wear resistance and corrosion resistance. Therefore, the surface roughness of machined thin walls was measured to evaluate the effects and efficiency of different machining strategies. As surface roughness also refers to the geometric characteristics on the surface, the topographies of the machined thin walls were observed and analysed as well. The average surface roughness (R_a) and surface morphologies of the thin walls machined under different machining environments are shown in Figs. 15 and 16, respectively.

From Fig. 15, it is noted that R_a is smaller when the CMQL temperature is lower. It is known that the surface roughness of the finished surface is largely influenced by the plasticity of the workpiece material [31, 49]. When the CMQL temperature and corresponding cutting temperature
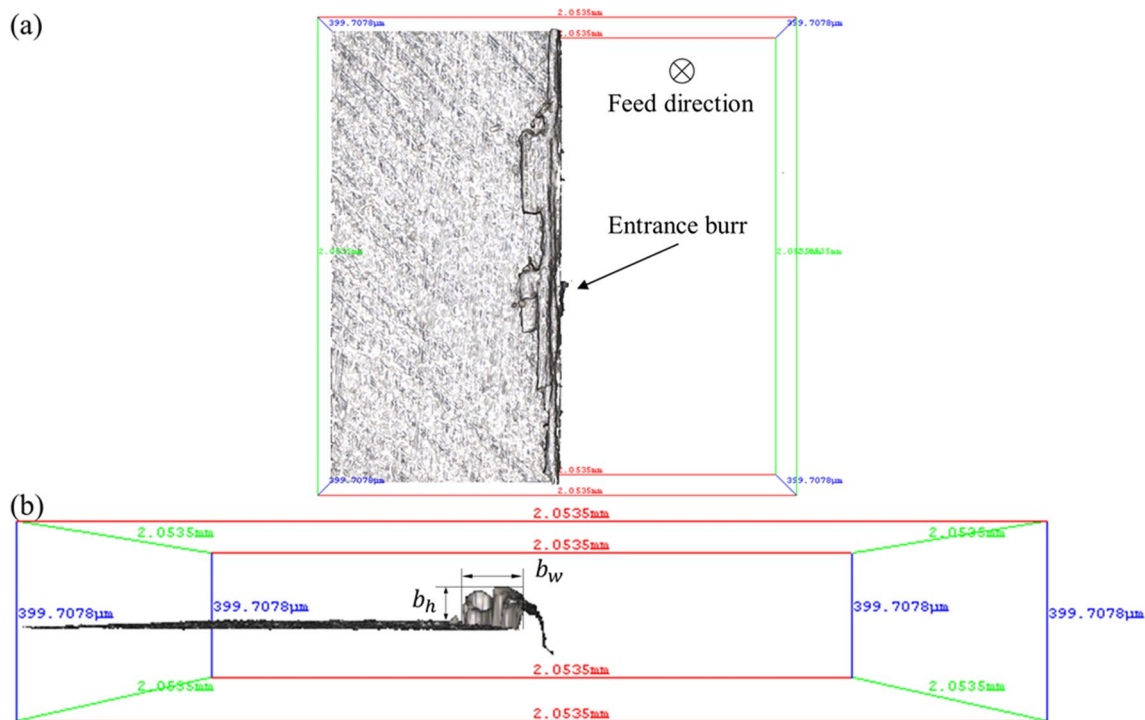

Fig. 11 a 3D topography image and b burr size measurement (MQL, $f_z = 0.06$ mm, $Vc = 113.10$ m/min, $a_e = 0.50$ mm, $a_p = 25$ mm)
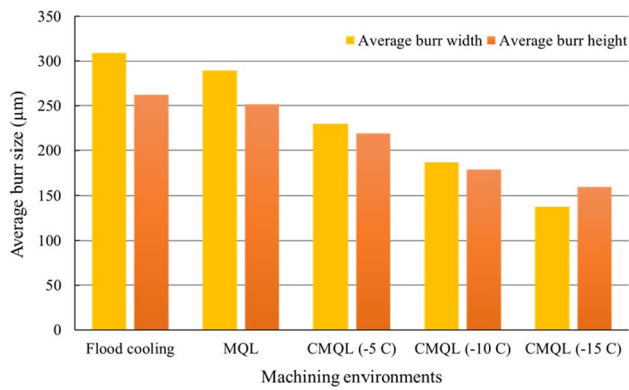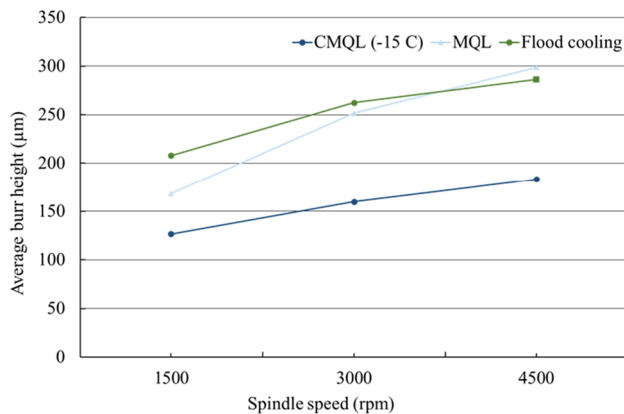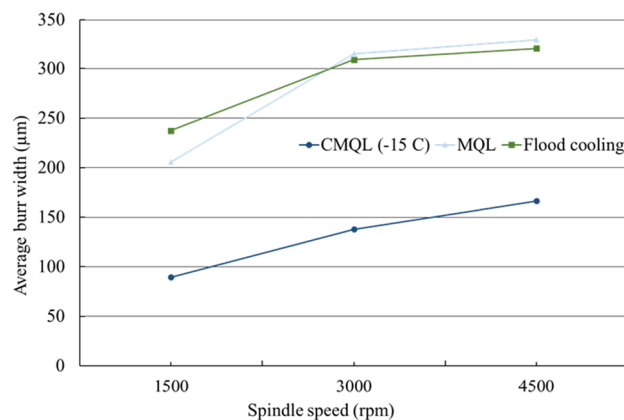
Fig. 12 Comparison of burr size under different machining environments ($f_z = 0.06$ mm, $Vc = 113.10$ m/min, $a_e = 0.50$ mm, $a_p = 25$ mm)

(a)

(b)

Fig. 13 Comparison of **a** burr height and **b** burr width under different machining conditions ($f_z = 0.06$ mm, $a_e = 0.50$ mm, $a_p = 25$ mm)

are lower, the plastic deformation ability of the material decreases, which is beneficial in preventing thermal distortion and chip adhesion. As the refrigerated mixture flow

also contributes to the maintenance of the formed lubrication film, the better lubrication performance and reduced cutting force make the machined surface significantly smoother. Therefore, the best surface quality is produced under CMQL (− 15 °C) condition, and the surface roughness was reduced by 16.53% and 23.46% in comparison to flood cooling and MQL.

The excessive thermomechanical loads generated during the milling of Ti-6Al-4 V can lead to the formation of undesirable defects on the finished surface. As shown in Fig. 16, noticeable scratch marks and adhesion are observed in flood cooling and MQL machining, which are caused by the discontinuous evacuation and re-welding of chips under severe cutting loads and pressure. Under MQL condition, there is even a swirled chip segment that is not completely removed from the machined surface (Fig. 15) due to a higher degree of adhesion. In addition, the presence of deep ridges and grooves indicates severe shear load, formation of BUE and extrusion of workpiece material under flood cooling and MQL conditions, while smearing marks are the result of large plastic deformation, formation of BUE on the tool edge and aggravated lubrication effect at higher cutting temperature.

Figure 16 e reveals that a much smoother surface with no obvious feed marks and other defects was obtained under the CMQL (− 15 °C) condition. Benefited by the strong heat transfer capacity and enhanced lubrication performance of CMQL (− 15 °C), the cutting loads are the lowest during the machining process, thereby the width difference of the ridges is the smallest, and no obvious uneven, adhesion or smearing occurred. Fewer scratch marks are found in CMQL (− 5 °C), but no scratch is observed in CMQL (− 10 °C) and CMQL (− 15 °C). This can be attributed to the easier separation of chips generated from the base material due to increased brittleness and decreased plasticity at lower cutting temperatures. Also, due to the working mechanism of the CMQL system, the flow rate and pressure of the mixture flow in CMQL are much higher than that in MQL, which helps to increase the penetration ability of the droplets, remove the chips more efficiently and prevent the recutting of generated chips.

Apart from the abovementioned surface defects, a common phenomenon is that noticeable vibration marks are found at the cut-in range (Fig. 17a), while intensive scratch and adhesion can be observed at the bottom area (Fig. 17b). In contrast, the machined surface in the middle and top areas is smoother and with fewer surface defects. The vibration mark is related to the suddenly increased chip load and transient vibration of the tool-workpiece system once the cutting edge is engaged with the workpiece material, while the scratch and adhesion defects are caused by the tool run-out or vibration, as well as chip jamming.
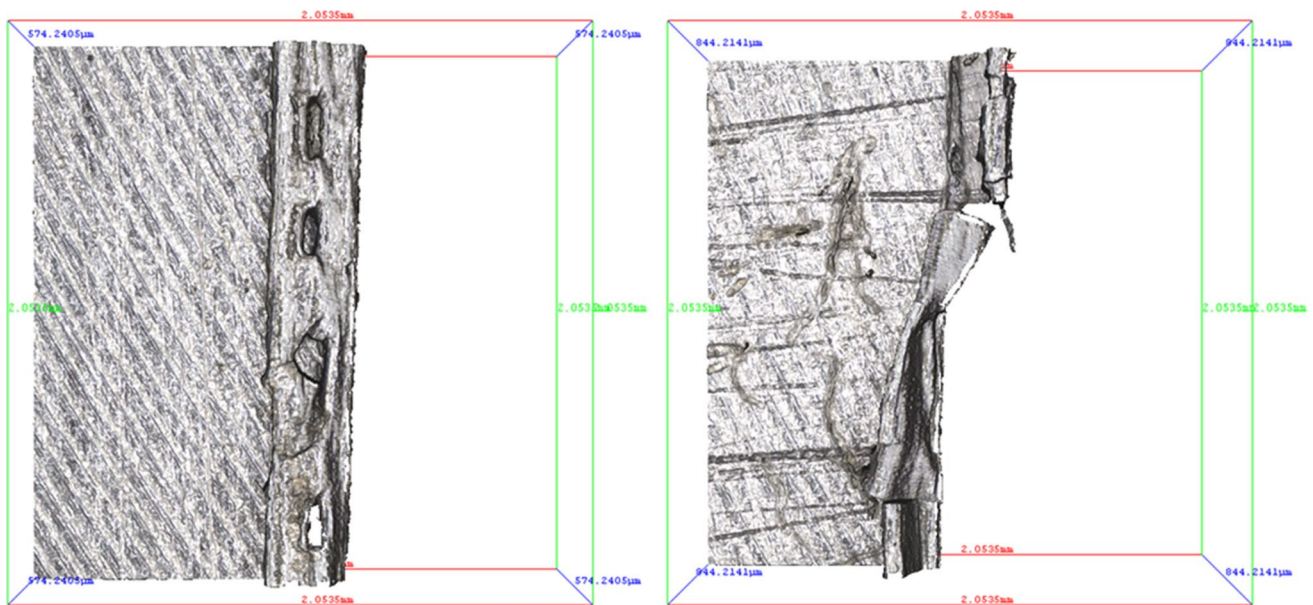
Fig. 14 Flat and irregular burr formation in MQL ($f_z = 0.06$ mm, $Vc = 169.65$ m/min, $a_e = 0.50$ mm, $a_p = 25$ mm)
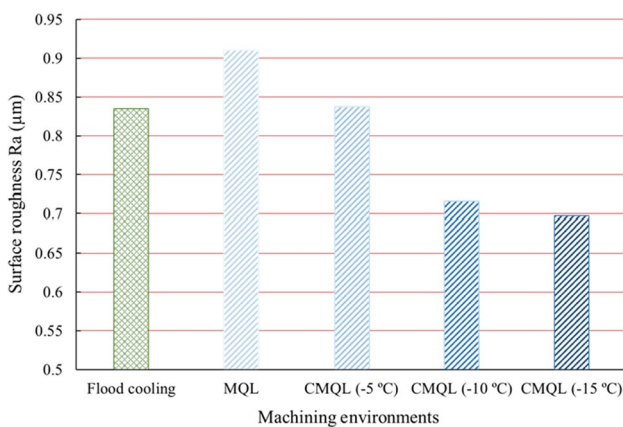

Fig. 15 Comparison of measured surface roughness between different machining environments ($f_z = 0.06$ mm, $a_e = 0.50$ mm, $a_p = 25$ mm, $n = 3000$ rpm)

Figures 18 and 19 summarise the measured R_a and surface morphologies of the machined surfaces under different machining conditions. It can be observed that the R_a decreased with the increasing spindle speed from 1500 to 3000 rpm and then increased at the spindle speed of 4500 rpm under both flood cooling and MQL conditions. In comparison, the CMQL (-15 °C) condition resulted in gradually decreased surface roughness and the lowest R_a, particularly at the highest spindle speed.

At lower spindle speed, it can be clearly found that the machined surfaces under flood cooling and MQL conditions appear to be very rough and irregular, and there are noticeable smearing, scratch, adhesion and deep furrows over the surfaces. But the MQL condition shows promoted surface finish than flood cooling due to better penetration and lubrication abilities of the atomised droplets, effective heat removal from the cutting zone through the rapid evaporation of the droplets and relatively lower cutting loads. At moderate spindle speed, the R_a decreases under all cutting conditions, which is mainly caused by a shorter deformation time, easier plastic deformation due to the intensive thermal softening effect and therefore reduced cutting force. According to the SEM images, there are also fewer defects occurring on the surfaces milled under flood cooling and MQL machining in comparison to the lower spindle speed condition.

However, at the spindle speed of 4500 rpm, deep scratches and intense adhesion are dominant in flood cooling and MQL machining respectively, as illustrated in Fig. 19. Because MQL is not able to provide adequate lubrication and cooling functions at higher spindle speed, the accelerated tool wear, sharply raised thermomechanical load and increasing ductility of workpiece material led to a large amount of lamellar adhesion over the machined surface. The serious adhesion on the surface and cutting edge would aggravate the chip evacuation, produce more cutting heat in the following cutting process and thus result in a rougher surface. Meanwhile, obvious smearing of the surface material is observed due to severe rubbing and ploughing actions of the cutting edge, which further suggests that both the lubrication and cooling functions of MQL are diminished during the machining.

Under CMQL (-15 °C) condition, the surface roughness always decreases with the increasing spindle speeds,
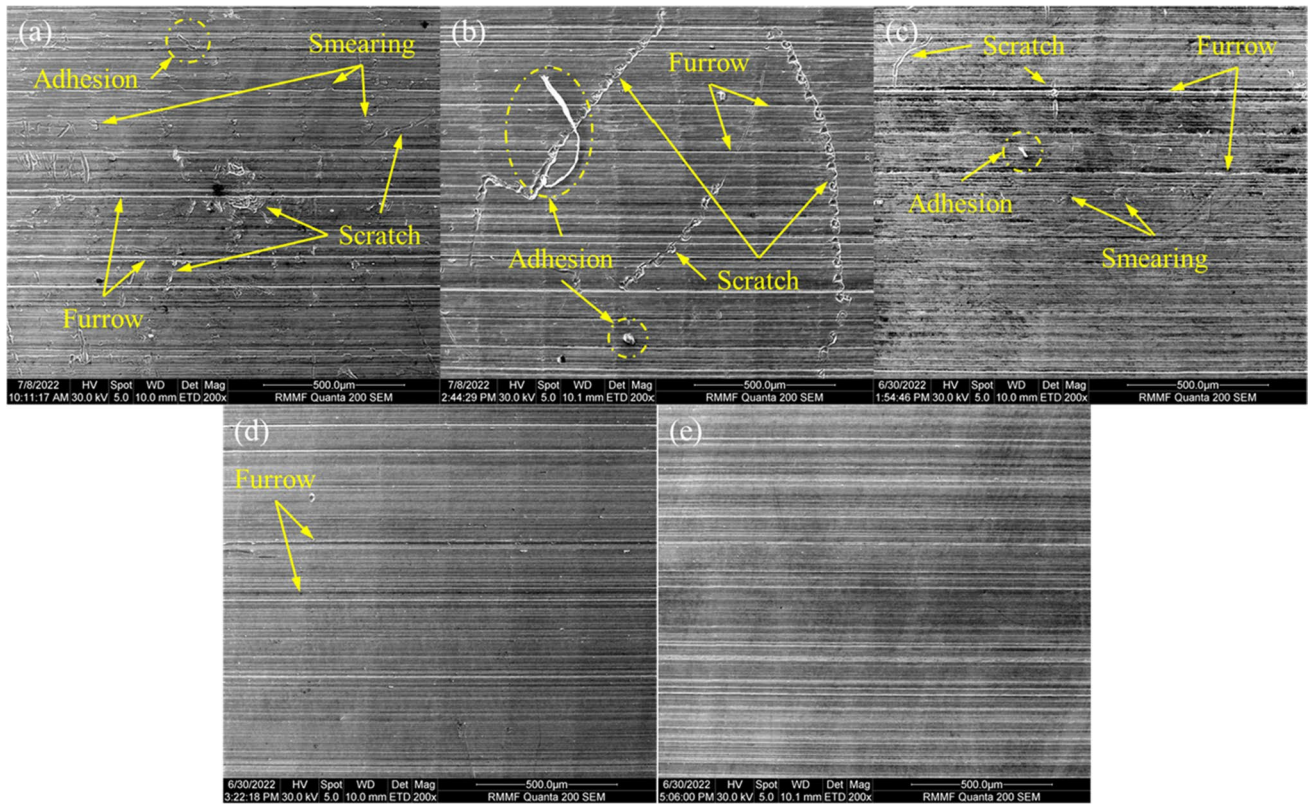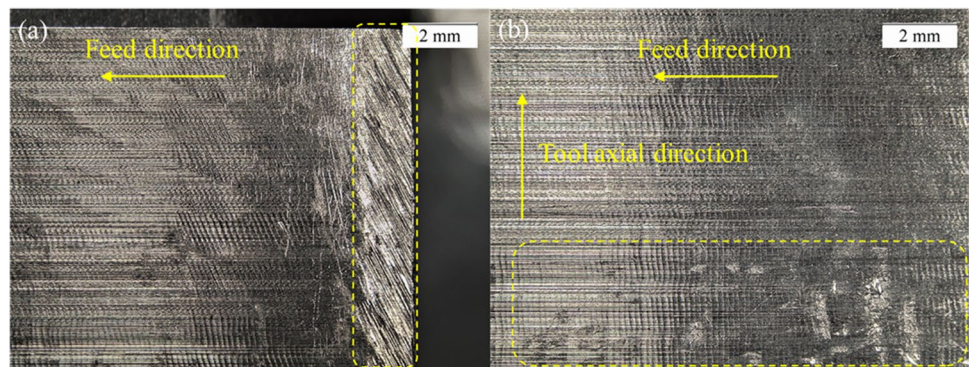
Fig. 16 Comparison of captured surface morphologies between different machining environments: **a** flood cooling, **b** MQL, **c** CMQL (-5 °C), **d** CMQL (-10 °C), **e** CMQL (-15 ℃) ($f_z = 0.06$ mm, $a_e = 0.50$ mm, $a_p = 25$ mm, $n = 3000$ rpm)

Fig. 17 Surface morphologies at the **a** cut-in and **b** bottom areas of machined surface (MQL, $f_z = 0.06$ mm, $Vc = 169.65$ m/min, $a_e = 0.50$ mm, $a_p = 25$ mm)

and smoother surfaces with few pronounced defects can be observed. At lower spindle speed, the surface shows only uniform distribution of tool trajectory parallel to the feed direction and slight scratch over the machined surface, as shown in Fig. 19. At moderate and the highest spindle speeds, it can be noted that the surface roughness values are considerably lower than that measured in flood cooling and MQL, and the surface texture appeared more complete and fairly uniform. The refrigerated compressed mixture flow accompanied by micro droplets contributed to a reduction of the cutting temperature, excessive friction and likelihood of chip jamming. Consequently, harder tool/workpiece material, mitigated adhesive/abrasive wear and less vibration resulted in improved surface quality to a large extent.

3.4 Comparison of surface form errors

In the milling process, elastic–plastic deformation of the flexible thin wall is almost inevitable due to the large length-to-thickness ratio and low rigidity of the part, as well as excessive cutting loads, which leads to varying part thickness and directly influences the functional performance of
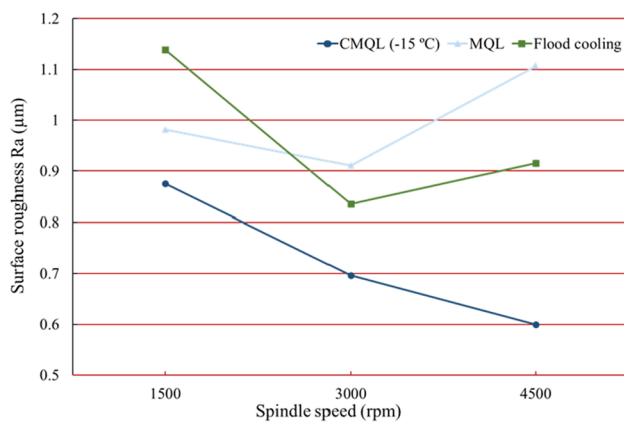
Fig. 18 Surface roughness measured at different machining conditions ($f_z = 0.06$ mm, $a_e = 0.50$ mm, $a_p = 25$ mm)

the machined part. Therefore, measuring and controlling cutting-induced deformation errors are essential to improve dimensional accuracy and productivity.

Figure 20 shows the side view of the machined thin wall. It is evident that the cutting-induced part deflection leads to surface form errors in both the feed and tool axial directions. To demonstrate the efficiency of CMQL machining, the maximum deflection values measured along the feed direction and under different machining conditions are compared in Figs. 21 and 22.

As shown in Fig. 21, the deflection changes nonlinearly along the feed direction due to the varying dynamic stiffness of the thin-wall part. In all cases, the deflection in the feed direction decreases first and then increases in the second half cutting process. And larger amplitudes of deflection occurred at the two ends of the thin wall (L1 and L3) due to lower stiffness of the part at these locations compared to the middle area (L2). In addition, due to the continuous material removal process, the rigidity of the part was much lower at the cut-out location (L3). Therefore, the maximum deformation was measured at L3. Moreover, it was noted that the deflection exhibited a decreasing tendency when the CMQL temperature decreased gradually.

Figure 22 indicates the reduction in part deflection with the increasing spindle speed due to the decreasing cutting force in the perpendicular direction. The cutting force and thermal load are considered to be the primary causes of thin-wall deformation [55, 56]. Larger cutting forces directly increase the magnitude of the deflection, while the complex and localised thermal stress distribution lead to non-uniform dimensional deviation of the machined part, which in turn affects the fatigue life and functional performance of machined thin walls. As CMQL machining outperformed other cutting strategies in reducing the coupling thermomechanical loads, this hybrid strategy owns obvious advantages in reducing the thin-wall deformation. Meanwhile, CMQL

machining also contributes to minimising the generation of additional machining-induced residual stresses that may lead to part distortion [57, 58]. And according to the investigation of [59, 60], the reduction of CMQL temperature level and corresponding thermal effect helps to inhibit the formation of tensile residual stress while producing higher compressive residual stresses within the machined part, which are beneficial for improving the fatigue strength of the thin-wall part. Therefore, CMQL can diminish the cutting-induced deformation and thermal distortion more efficiently than flood cooling and MQL. When the spindle speed was 1500 rpm, the machined thin-wall part from CMQL (-15 °C) exhibited 56.97% and 32.51% lower deflection value in comparison to flood cooling and MQL machining, respectively. In addition, considering the reduced part deformation but deteriorated tool wear resistance and surface finish at higher spindle speeds, CMQL machining can perform a prominent role in the machining of titanium thin-wall components by increasing productivity and quality while inhibiting the part deformation.

Due to the occurrence of part deflection and varying tool-workpiece engagement conditions, partial workpiece material cannot be properly removed as planned. Therefore, thickness errors of the finished part are formed along both the feed and height directions. Figure 23 shows the absolute thickness errors measured at selected locations.

According to Fig. 23b, the thickness of the machined part is not uniform along the feed and height directions, and a common tendency is that larger absolute thickness errors are found around the free ends of the part. Compared to the constrained bottom edge of the thin-wall part, the top edge with smaller rigidity resulted in more significant elastic–plastic deflection, reduced radial depth of cutting and the amount of material removal. Therefore, the thickness error decreased gradually from the top to the bottom edge. Also, due to the decreasing stiffness and increasing deflection of the thin-wall part during the following cutting process, the minimum instantaneous uncut chip thickness and the maximum absolute thickness errors appeared at the top end side of the machined thin wall.

Figure 24 presents the average absolute thickness errors regarding different cutting conditions. The absolute errors of the machined part under CMQL (-15 °C) condition are always smaller than that calculated under other cutting conditions, and relatively less variation of absolute error is observed in CMQL (-15 °C). Based on the above-mentioned experimental results, it can be seen that the CMQL (-15 °C) condition results in a more stable cutting process with fewer surface form errors due to reduced thermomechanical loads and chip load variation. Therefore, the thin-wall part machined under CMQL (-15 °C) condition is more uniform, and at the spindle speed of 3000 rpm, the maximum thickness error in CMQL (-15 °C) among the
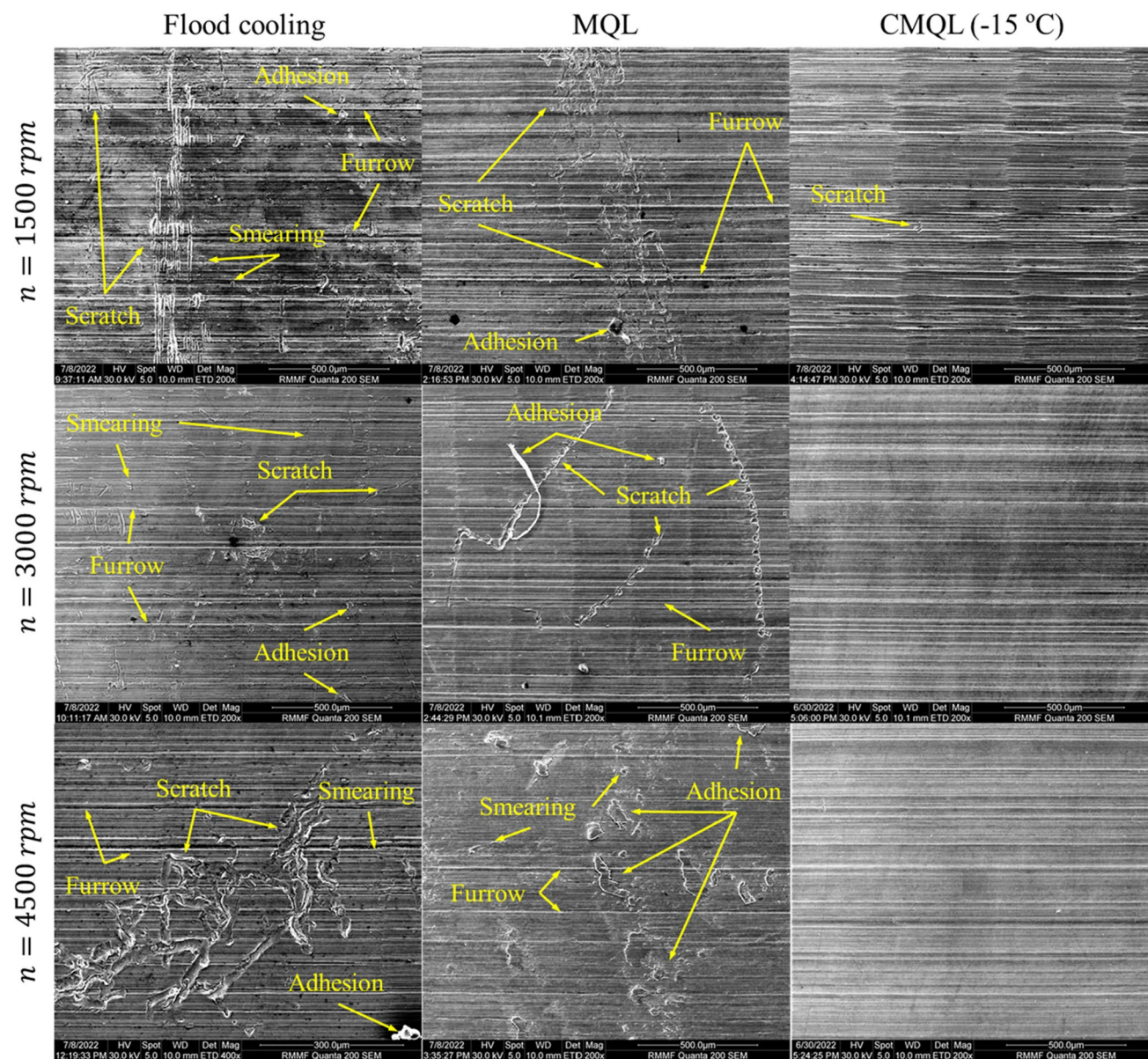
Fig. 19 Surface morphologies captured at different machining conditions ($f_z = 0.06$ mm, $a_e = 0.50$ mm, $a_p = 25$ mm)

selected positions is about 53.51% and 20.56% smaller than that in flood cooling and MQL machining.

3.5 Sustainability and limitations

According to experimental results, conventional flood cooling strategy has provided a more stable performance under varying cutting conditions compared with MQL. The abundant amount of MWF used in this strategy offsets the reduced cooling/lubrication efficiency in high-speed machining of titanium alloy. However, the implementation of flood cooling method and MWF has become a general concern due to the significant environmental, health and machining cost issues. MQL is considered a green and sustainable machining strategy as a very small amount of MWF is required while impressive machining quality can be achieved. But the inadequate functional performance of MQL limits its application in high-speed machining of difficult-to-machine materials. The investigations of cryogenic machining that uses mediums such as LCO_2 and LN_2 have been proven to be efficient in improving tool life and surface finish. And this cooling/lubrication strategy has been considered highly sustainable with less carbon emissions and machining costs compared to dry machining [61, 62]. However, the pre-treatment, transportation, storage and disposal of the cryogenic mediums would result in additional machining costs.
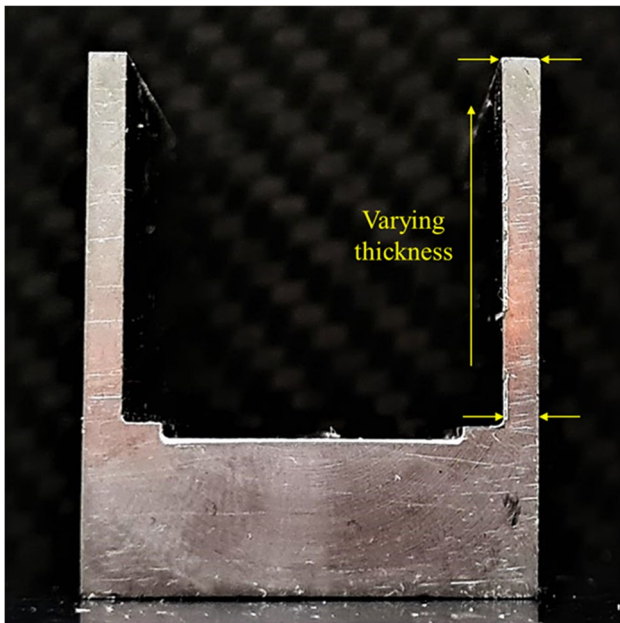
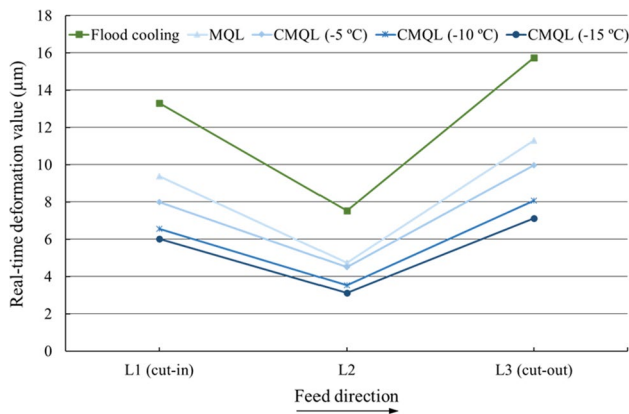**Fig. 20** Side view of the deformed thin-wall part

Fig. 21 Comparison of maximum deflection values along the feed direction ($f_z = 0.06$ mm, $Vc = 113.10$ m/min, $a_e = 0.50$ mm, $a_p = 25$ mm)

Fig. 22 Comparison of maximum deflection values under different machining conditions ($f_z = 0.06$ mm, $a_e = 0.50$ mm, $a_p = 25$ mm)

Fig. 23 a Measurement scheme and **b** absolute thickness errors of the thin-wall parts (MQL, $f_z = 0.06$ mm, $Vc = 113.10$ m/min, $a_e = 0.50$ mm, $a_p = 25$ mm)

As a sustainable alternative to flood cooling strategy, CMQL promotes a hazardless and environment-friendly machining process. The consumption of MWF in CMQL is much smaller, which leads to significant eco-benefit. Meanwhile, reduced cutting loads and easier material removal during the cutting process result in reduced power consumption and increased productivity. In addition, the mitigated tool wear and increased tool rigidity under CMQL condition can also minimise the total machining cost. The finished thin-wall part with fewer surface defects and surface form errors further reduces the cost associated with post-processing operations such as deburring and grinding.
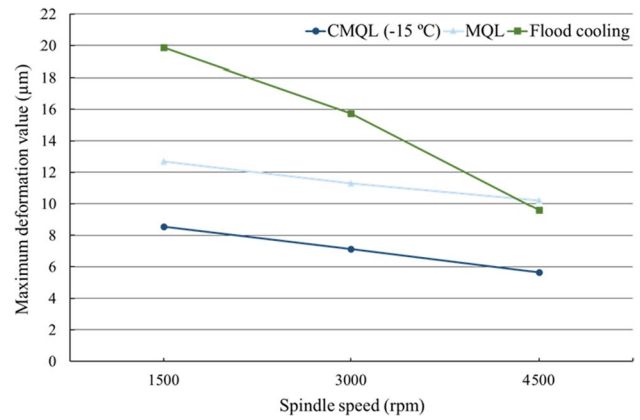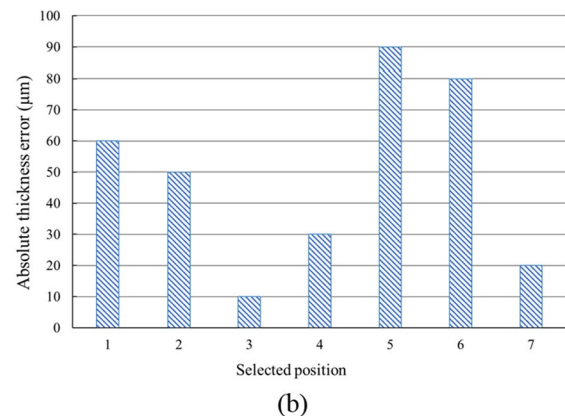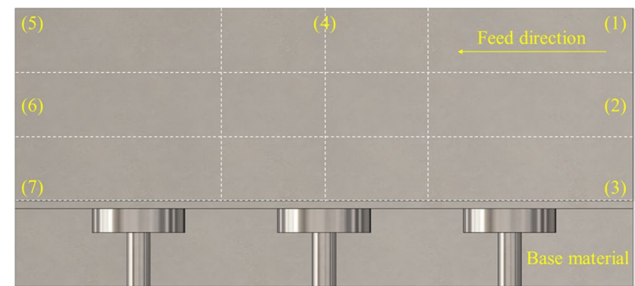
However, it should be noted that a large airflow volume is required for the generation of the refrigerated airflow in CMQL. And a lower flow temperature requires a higher flow rate, resulting in extra power consumption for the air compressor. Meanwhile, the performance of CMQL does not always increase with the decreasing flow temperature due to the varying physical properties and atomization characteristics of the base MWF. The constantly decreasing
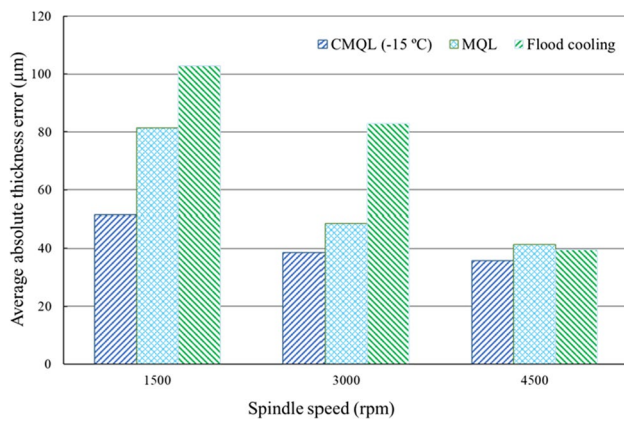
Fig. 24 Absolute thickness errors of the thin-wall parts machined under different machining conditions (f_z = 0.06 mm, a_e = 0.50 mm, a_p = 25 mm)

flow temperature would result in higher viscosity of the MWF, therefore, smaller area-to-volume ratio, larger surface tension and contact angle of the droplets, which can cause adverse effects on the penetrability, wettability and film-forming ability. So, the flow temperature and viscosity of the droplets should be well-balanced. Moreover, the decreasing flow temperature causes a large temperature gradient and periodic thermal stress along the cutting edge, adversely affecting the mechanical properties of the tool and tool life. And an excessive cooling environment can also lead to increased yield stresses and work hardening of the workpiece material, and therefore larger cutting forces are required for removing the material.

Considering the above-mentioned issues and the sustainability of CMQL, it is necessary to optimise and determine the most reasonable temperature range that allows maximum material removal rate and minimum surface form errors while keeping acceptable power consumption.

4 Conclusions

In this work, Ti-6Al-4 V thin-wall milling experiments under flood cooling, MQL and CMQL conditions were conducted to explore the mechanisms and performance of CMQL as a sustainable machining strategy. The results show that different machining environments greatly influence the cutting forces, tool wear state, surface integrity and surface form errors. The following conclusions can be reached from the investigations:

(1) In machining Ti-6Al-4 V thin-wall parts, the generation and accumulation of cutting heat are more severe under higher MRR conditions. It results in high chemical reactivity of the tool-workpiece material pair, significant

thermal softening and complex thermal stress distribution. Meanwhile, the cooling and lubrication effects are interrelated and mutually influenced. Therefore, efficient cooling capacity of the applied cooling/lubrication method becomes more important in high-speed machining of titanium alloys.

(2) The experimental results indicate the fundamental effect of MQL is lubrication, and it has a better performance than flood cooling at lower spindle speeds. However, the cooling/lubrication capacities of MQL are inadequate and degraded when the spindle speed exceeds a certain level (4500 rpm in this study), which is the primary reason of the seriously deteriorated tool wear state and the formation of burr.

(3) Within a certain range, a lower CMQL temperature level is advantageous to producing better wear resistance and lower thermomechanical loads, which are attributed to the enlarged temperature difference and enhanced cooling capacity through forced convection and boiling heat transfer of the refrigerated mixture flow. And a more stable lubrication film through the increased absorbability and bearing ability of the micro droplets, even at higher spindle speeds. The high-pressure flow also facilitates better atomization and penetration of the droplets, as well as effective breaking and evacuation of generated chips, which consequently reduces the cutting loads and prevents surface damage. Therefore, CMQL is beneficial to the high-speed machining of titanium alloys.

(4) CMQL (− 15 °C) results in remarkable improvement in the machinability of titanium thin-wall parts, even at higher cutting velocities. The cutting temperature and thermal softening effect are inhibited more effectively than flood cooling and MQL, and the conditions of adhesion wear, burr formation, surface finish and thermal expansion are controlled considerably. It has also been proved that CMQL (− 15 °C) provides a better lubrication effect along the contact interfaces and results in diminished flank wear and defects over the machined surfaces.

(5) Due to a more stable cutting process and mitigated thermal–mechanical cutting loads under CMQL (− 15 °C) condition, the finished thin walls are more uniform and with improved dimensional accuracy. The results show that when the spindle speed was 3000 rpm, the maximum deflection value was reduced by 54.74% and 36.99%, while the maximum thickness error was about 53.51% and 20.56% smaller in comparison to flood cooling and MQL.

(6) The efficiency of different cooling/lubrication strategies largely depends on the milling parameters such as the spindle speed and CMQL parameters such as the flow pressure. Therefore, the optimal CMQL parameters should be further identified according to the designed cutting parameters.

(7) Benefiting from the superior performance of CMQL, the cutting velocity or spindle speed could be further increased to achieve a higher productivity. Meanwhile, the overall machining costs of MWF, cutting tools and subsequent post-process can be reduced or even eliminated in comparison with conventional flood cooling and MQL machining. Moreover, CMQL does not require specialized store and transfer systems, providing both economic and environmental benefits to the operation. Therefore, CMQL machining promotes a cleaner and sustainable production process and a more comprehensive application of titanium thin-wall components in industries.

Declarations

Ethics approval The authors state that the submitted work is original, the manuscript in part or in full has not been submitted or published anywhere, and it will not be submitted elsewhere until the editorial process is completed. The authors affirm that the results are presented without fabrication and ensure that all the authors mentioned in the manuscript have agreed to authorship, read and approved the manuscript, and given consent for submission and subsequent publication. All named authors agree on the order of authorship.

Consent to participate Not applicable.

Consent for publication The authors grant the publisher permission to publish the work entitled Accurate vibration-free robotic milling electric discharge machining. The author properly authorises its dissemination in various forms and permits the conversion of the work into machine-readable form and storage of the work in electronic databases.

Conflict of interest The authors declare no competing interests.

References

1. Pramanik A (2014) Problems and solutions in machining of titanium alloys. Int J Adv Manuf Technol 70(5):919–928. https://doi.org/10.1007/s00170-013-5326-x

2. Rao CM, Rao SS, Herbert MA (2018) Development of novel cutting tool with a micro-hole pattern on PCD insert in machining of titanium alloy. J Manuf Process 36:93–103. https://doi.org/10.1016/j.jmapro.2018.09.028

3. Budak E, Altintas Y (1995) Modeling and avoidance of static form errors in peripheral milling of plates. Int J Mach Tools Manuf 35(3):459–476. https://doi.org/10.1016/0890-6955(94)P2628-S

4. Ding SL, Izamshah RA R, Mo J, Zhu YW (2011) Chatter detection in high speed machining of titanium alloys. In: Key Engineering Materials. Trans Tech Publ, pp 289–294. https://doi.org/10.4028/www.scientific.net/KEM.458.289

5. Li Z-L, Tuysuz O, Zhu L-M, Altintas Y (2018) Surface form error prediction in five-axis flank milling of thin-walled parts. Int J Mach Tools Manuf 128:21–32. https://doi.org/10.1016/j.ijmachtools.2018.01.005

6. Del Sol I, Rivero A, López de Lacalle LN, Gamez AJ (2019) Thin-wall machining of light alloys: A review of models and industrial approaches. Materials 12(12):2012. https://doi.org/10.3390/ma12122012

7. Altintas Y, Stepan G, Budak E, Schmitz T, Kilic ZM (2020) Chatter stability of machining operations. J Manuf Sci Eng 142(11). https://doi.org/10.1115/1.4047391

8. Wu G, Li G, Pan W, Raja I, Wang X, Ding S (2021) A state-of-art review on chatter and geometric errors in thin-wall machining processes. J Manuf Process 68:454–480. https://doi.org/10.1016/j.jmapro.2021.05.055

9. Kang Y-G, Wang Z-Q (2013) Two efficient iterative algorithms for error prediction in peripheral milling of thin-walled workpieces considering the in-cutting chip. Int J Mach Tools Manuf 73:55–61. https://doi.org/10.1016/j.ijmachtools.2013.06.001

10. Sun Y, Jiang S (2018) Predictive modeling of chatter stability considering force-induced deformation effect in milling thin-walled parts. Int J Mach Tools Manuf 135:38–52. https://doi.org/10.1016/j.ijmachtools.2018.08.003

11. Wang X, Li Z, Bi Q, Zhu L, Ding H (2019) An accelerated convergence approach for real-time deformation compensation in large thin-walled parts machining. Int J Mach Tools Manuf 142:98–106. https://doi.org/10.1016/j.ijmachtools.2018.12.004

12. Altintas Y, Stépán G, Merdol D, Dombóvári Z (2008) Chatter stability of milling in frequency and discrete time domain. CIRP J Manuf Sci Technol 1(1):35–44. https://doi.org/10.1016/j.cirpj.2008.06.003

13. Feng J, Wan M, Gao T-Q, Zhang W-H (2018) Mechanism of process damping in milling of thin-walled workpiece. Int J Mach Tools Manuf 134:1–19. https://doi.org/10.1016/j.ijmachtools.2018.06.001

14. Tuysuz O, Altintas Y (2017) Frequency domain updating of thin-walled workpiece dynamics using reduced order substructuring method in machining. J Manuf Sci Eng 139(7). https://doi.org/10.1115/1.4036124

15. Pan W, Kamaruddin A, Ding S, Mo J (2014) Experimental investigation of end milling of titanium alloys with polycrystalline diamond tools. Proc Inst Mech Eng B: J Eng Manuf 228(8):832–844. https://doi.org/10.1177/0954405413514399

16. Iskandar Y, Tendolkar A, Attia M, Hendrick P, Damir A, Diakodimitris C (2014) Flow visualization and characterization for optimized MQL machining of composites. CIRP Ann 63(1):77–80. https://doi.org/10.1016/j.cirp.2014.03.078

17. Sharma J, Sidhu BS (2014) Investigation of effects of dry and near dry machining on AISI D2 steel using vegetable oil. J

Clean Prod 66:619–623. https://doi.org/10.1016/j.jclepro.2013.11.042

18. Rahman M, Kumar AS, Salam M (2002) Experimental evaluation on the effect of minimal quantities of lubricant in milling. Int J Mach Tools Manuf 42(5):539–547. https://doi.org/10.1016/S0890-6955(01)00160-2

19. Liao Y, Lin H, Chen Y (2007) Feasibility study of the minimum quantity lubrication in high-speed end milling of NAK80 hardened steel by coated carbide tool. Int J Mach Tools Manuf 47(11):1667–1676. https://doi.org/10.1016/j.ijmachtools.2007.01.005

20. Li K-M, Chou S-Y (2010) Experimental evaluation of minimum quantity lubrication in near micro-milling. J Mater Process Technol 210(15):2163–2170. https://doi.org/10.1016/j.jmatprotec.2010.07.031

21. Fratila D, Caizar C (2011) Application of Taguchi method to selection of optimal lubrication and cutting conditions in face milling of AlMg3. J Clean Prod 19(6–7):640–645. https://doi.org/10.1016/j.jclepro.2010.12.007

22. Yuan S, Yan L, Liu W, Liu Q (2011) Effects of cooling air temperature on cryogenic machining of Ti-6Al-4V alloy. J Mater Process Technol 211(3):356–362. https://doi.org/10.1016/j.jmatprotec.2010.10.009

23. Leppert T (2011) Effect of cooling and lubrication conditions on surface topography and turning process of C45 steel. Int J Mach Tools Manuf 51(2):120–126. https://doi.org/10.1016/j.ijmachtools.2010.11.001

24. Daniel DM, Moraes DLd, Garcia MV, Lopes JC, Rodriguez RL, Ribeiro FSF, Sanchez LEdA, Bianchi EC (2023) Application of MQL with cooled air and wheel cleaning jet for greener grinding process. Int J Adv Manuf Technol 125(1–2):435–452. https://doi.org/10.1007/s00170-022-10712-3

25. Liu F, Wu X, Xia Y, Lv T, Zhang R, Hu X, Xu X (2023) A novel cold air electrostatic minimum quantity lubrication (CAEMQL) technique for the machining of titanium alloys Ti-6Al-4V. Int J Adv Manuf Technol 126(7–8):3437–3452. https://doi.org/10.1007/s00170-023-11222-6

26. Yong H, Sun YJ, Ge MJ, Li JF, Sun J (2011) Milling experimental investigation on titanium alloy Ti6Al4V under different cooling/lubrication conditions. In: Advanced Materials Research. Trans Tech Publ, pp 406–411. https://doi.org/10.4028/www.scientific.net/AMR.325.406

27. Truesdale SL, Shin YC (2009) Microstructural analysis and machinability improvement of Udimet 720 via cryogenic milling. Mach Sci Technol 13(1):1–19. https://doi.org/10.1080/10910340902776010

28. Shokrani A, Al-Samarrai I, Newman ST (2019) Hybrid cryogenic MQL for improving tool life in machining of Ti-6Al-4V titanium alloy. J Manuf Process 43:229–243. https://doi.org/10.1016/j.jmapro.2019.05.006

29. Yang Q, Wang B, Deng J, Zheng Y, Kong X (2022) The effect of addition of MWCNT nanoparticles to CryoMQL conditions on tool wear patterns, tool life, roughness, and temperature in turning of Ti-6Al-4V. Int J Adv Manuf Technol 120(7–8):5587–5604. https://doi.org/10.1007/s00170-022-09101-7

30. Pereira O, Català P, Rodríguez A, Ostra T, Vivancos J, Rivero A, López-de-Lacalle LN (2015) The use of hybrid CO2+MQL in machining operations. Procedia engineering 132:492–499. https://doi.org/10.1016/j.proeng.2015.12.524

31. Shokrani A, Dhokia V, Newman ST (2016) Investigation of the effects of cryogenic machining on surface integrity in CNC end milling of Ti-6Al-4V titanium alloy. J Manuf Process 21:172–179. https://doi.org/10.1016/j.jmapro.2015.12.002

32. Sun S, Brandt M, Dargusch M (2010) Machining Ti-6Al-4V alloy with cryogenic compressed air cooling. Int J Mach Tools Manuf 50(11):933–942. https://doi.org/10.1016/j.ijmachtools.2010.08.003

33. Zhang S, Li J, Wang Y (2012) Tool life and cutting forces in end milling Inconel 718 under dry and minimum quantity cooling lubrication cutting conditions. J Clean Prod 32:81–87. https://doi.org/10.1016/j.jclepro.2012.03.014

34. Benjamin DM, Sabarish VN, Hariharan M, Raj DS (2018) On the benefits of sub-zero air supplemented minimum quantity lubrication systems: an experimental and mechanistic investigation on end milling of Ti-6-Al-4-V alloy. Tribol Int 119:464–473. https://doi.org/10.1016/j.triboint.2017.11.021

35. Bagherzadeh A, Kuram E, Budak E (2021) Experimental evaluation of eco-friendly hybrid cooling methods in slot milling of titanium alloy. J Clean Prod 289:125817. https://doi.org/10.1016/j.jclepro.2021.125817

36. Yi S, Li G, Ding S, Mo J (2017) Performance and mechanisms of graphene oxide suspended cutting fluid in the drilling of titanium alloy Ti-6Al-4V. J Manuf Process 29:182–193. https://doi.org/10.1016/j.jmapro.2017.07.027

37. Hegab H, Umer U, Deiab I, Kishawy H (2018) Performance evaluation of Ti-6Al-4V machining using nano-cutting fluids under minimum quantity lubrication. Int J Adv Manuf Technol 95(9):4229–4241. https://doi.org/10.1007/s00170-017-1527-z

38. Wu G, Li G, Pan W, Raja I, Wang X, Ding S (2022) Experimental investigation of eco-friendly cryogenic minimum quantity lubrication (CMQL) strategy in machining of Ti-6Al-4V thin-wall part. J Clean Prod 357:131993. https://doi.org/10.1016/j.jclepro.2022.131993

39. Maruda RW, Krolczyk GM, Feldshtein E, Pusavec F, Szydlowski M, Legutko S, Sobczak-Kupiec A (2016) A study on droplets sizes, their distribution and heat exchange for minimum quantity cooling lubrication (MQCL). Int J Mach Tools Manuf 100:81–92. https://doi.org/10.1016/j.ijmachtools.2015.10.008

40. Liu N-M, Chiang K-T, Hung C-M (2013) Modeling and analyzing the effects of air-cooled turning on the machinability of Ti-6Al-4V titanium alloy using the cold air gun coolant system. Int J Adv Manuf Technol 67(5):1053–1066. https://doi.org/10.1007/s00170-012-4547-8

41. Li G, Yi S, Li N, Pan W, Wen C, Ding S (2019) Quantitative analysis of cooling and lubricating effects of graphene oxide nanofluids in machining titanium alloy Ti6Al4V. J Mater Process Technol 271:584–598. https://doi.org/10.1016/j.jmatprotec.2019.04.035

42. Yi S, Li N, Solanki S, Mo J, Ding S (2019) Effects of graphene oxide nanofluids on cutting temperature and force in machining Ti-6Al-4V. Int J Adv Manuf Technol 103(1):1481–1495. https://doi.org/10.1007/s00170-019-03625-1

43. Saini S, Ahuja IS, Sharma VS (2012) Residual stresses, surface roughness, and tool wear in hard turning: a comprehensive review. Mater Manuf Processes 27(6):583–598. https://doi.org/10.1080/10426914.2011.585505

44. Zhang Y, Li C, Yang M, Jia D, Wang Y, Li B, Hou Y, Zhang N, Wu Q (2016) Experimental evaluation of cooling performance by friction coefficient and specific friction energy in nanofluid minimum quantity lubrication grinding with different types of vegetable oil. J Clean Prod 139:685–705. https://doi.org/10.1016/j.jclepro.2016.08.073

45. Lin H, Wang C, Yuan Y, Chen Z, Wang Q, Xiong W (2015) Tool wear in Ti-6Al-4V alloy turning under oils on water cooling comparing with cryogenic air mixed with minimal quantity lubrication. Int J Adv Manuf Technol 81(1):87–101. https://doi.org/10.1007/s00170-015-7062-x

46. Ding S, Yang D, Han Z (2005) Boundary-conformed machining of turbine blades. Proc Inst Mech Eng B: J Eng Manuf 219(3):255–263. https://doi.org/10.1243/095440505X28981

47. Yang DC, Chuang J, Han Z, Ding S (2003) Boundary-conformed toolpath generation for trimmed free-form surfaces via Coons reparametrization. J Mater Process Technol 138(1–3):138–144. https://doi.org/10.1016/S0924-0136(03)00062-1

48. Park K-H, Suhaimi MA, Yang G-D, Lee D-Y, Lee S-W, Kwon P (2017) Milling of titanium alloy with cryogenic cooling and minimum quantity lubrication (MQL). Int J Precis Eng Manuf 18(1):5–14. https://doi.org/10.1007/s12541-017-0001-z

49. An Q, Dang J (2020) Cooling effects of cold mist jet with transient heat transfer on high-speed cutting of titanium alloy. Int J Precis Eng Manuf-Green Technol 7(2):271–282. https://doi.org/10.1007/s40684-019-00076-7

50. Li G, Li N, Wen C, Ding S (2018) Investigation and modeling of flank wear process of different PCD tools in cutting titanium alloy Ti6Al4V. Int J Adv Manuf Technol 95(1):719–733. https://doi.org/10.1007/s00170-017-1222-0

51. Li G, Rahim MZ, Pan W, Wen C, Ding S (2020) The manufacturing and the application of polycrystalline diamond tools-a comprehensive review. J Manuf Process 56:400–416. https://doi.org/10.1016/j.jmapro.2020.05.010

52. Pan W, Ding S, Mo J (2014) Thermal characteristics in milling Ti6Al4V with polycrystalline diamond tools. Int J Adv Manuf Technol 75(5):1077–1087. https://doi.org/10.1007/s00170-014-6094-y

53. Li G, Yi S, Wen C, Ding S (2018) Wear mechanism and modeling of tribological behavior of polycrystalline diamond tools when cutting Ti6Al4V. J Manuf Sci Eng 140(12). https://doi.org/10.1115/1.4041327

54. Rahman M, Senthil Kumar A (2001) Evaluation of minimal of lubricant in end milling. Int J Adv Manuf Technol 18(4):235–241. https://doi.org/10.1007/s001700170063

55. Bolar G, Joshi SN (2017) Three-dimensional numerical modeling, simulation and experimental validation of milling of a thin-wall component. Proc Inst Mech Eng B: J Eng Manuf 231(5):792–804. https://doi.org/10.1177/0954405416685387

56. Wu G, Li G, Pan W, Wang X, Ding S (2020) A prediction model for the milling of thin-wall parts considering thermal-mechanical coupling and tool wear. Int J Adv Manuf Technol 107(11):4645–4659. https://doi.org/10.1007/s00170-020-05346-2

57. Schajer GS, Ruud CO (2013) Overview of residual stresses and their measurement. Practical residual stress measurement methods. pp 1–27. https://doi.org/10.1002/9781118402832.ch1

58. Huang X, Sun J, Li J (2015) Effect of initial residual stress and machining-induced residual stress on the deformation of aluminium alloy plate. Stroj Vestn/J Mech Eng 61(2). https://doi.org/10.5545/sv-jme.2014.1897

59. Withers PJ, Bhadeshia H (2001) Residual stress. Part 2-Nature and origins. Mater Sci Technol 17(4):366–375. https://doi.org/10.1179/026708301101510087

60. Manimaran G, Anwar S, Rahman MA, Korkmaz ME, Gupta MK, Alfaify A, Mia M (2021) Investigation of surface modification and tool wear on milling Nimonic 80A under hybrid lubrication. Tribol Int 155:106762. https://doi.org/10.1016/j.triboint.2020.106762

61. Ross NS, Ganesh M, Srinivasan D, Gupta MK, Korkmaz ME, Krolczyk J (2022) Role of sustainable cooling/lubrication conditions in improving the tribological and machining characteristics of Monel-400 alloy. Tribol Int 176:107880. https://doi.org/10.1016/j.triboint.2022.107880

62. Khanna N, Airao J, Kshitij G, Nirala CK, Hegab H (2023) Sustainability analysis of new hybrid cooling/lubrication strategies during machining Ti6Al4V and Inconel 718 alloys. Sustain Mater Technol 36:e00606. https://doi.org/10.1016/j.susmat.2023.e00606